

Google Earth: A New Resource for Shoreline Change Estimation—Case Study from Jaffna Peninsula, Sri Lanka

T. W. S. Warnasuriya, Kuddithamby Gunaalan & S. S. Gunasekara

To cite this article: T. W. S. Warnasuriya, Kuddithamby Gunaalan & S. S. Gunasekara (2018) Google Earth: A New Resource for Shoreline Change Estimation—Case Study from Jaffna Peninsula, Sri Lanka, *Marine Geodesy*, 41:6, 546-580, DOI: [10.1080/01490419.2018.1509160](https://doi.org/10.1080/01490419.2018.1509160)

To link to this article: <https://doi.org/10.1080/01490419.2018.1509160>



Published online: 26 Oct 2018.



Submit your article to this journal [↗](#)



Article views: 818



View related articles [↗](#)



View Crossmark data [↗](#)



Citing articles: 7 View citing articles [↗](#)



Google Earth: A New Resource for Shoreline Change Estimation—Case Study from Jaffna Peninsula, Sri Lanka

T. W. S. Warnasuriya^a , Kuddithamby Gunaalan^b, and S. S. Gunasekara^c

^aFaculty of Fisheries and Ocean Sciences, Ocean University of Sri Lanka, Tangalle, Sri Lanka;

^bFaculty of Science, Department of Fisheries Science, University of Jaffna, Jaffna, Sri Lanka;

^cNational Aquatic Resources Research and Development Agency, Colombo, Sri Lanka

ABSTRACT

Estimation of shoreline change using satellite images is considered as a very effective method because the coastline is found highly dynamic. This study focuses to develop a methodology to detect shoreline changes using satellite imageries obtained from Google Earth platform. The study was carried out in north-east coastline of Jaffna in Sri Lanka. Shorelines from 2002 to 2017 were delineated on the multi-temporal satellite images in the Google Earth software by visual interpretation and change was detected using Digital Shoreline Analysis System in ArcGIS. Tidal variation, digitizing error, and geometric errors were considered to calculate the uncertainty. Mean End Point Rate, mean Shoreline Change Envelop, mean Net Shoreline Movement, and mean Weighted Linear Regression Rate were used as main shoreline change statistics. Result shows that there is net shoreline accretion of 6.13 ± 8.74 m with an annual rate of deposition of 0.5 m/year. During the study period, 76.12% of the observed shoreline is found accreted while the 23.88% of the shoreline is eroded. Mean Uncertainty of the shoreline is 3.73 ± 0.59 m. The study revealed that the satellite images from Google Earth platform can be used for time series analysis of shorelines after appropriate corrections.

ARTICLE HISTORY

Received 14 November 2017
Accepted 31 July 2018

KEYWORDS

GIS; Google earth platform;
DSAS; remote sensing;
shoreline change

Introduction

When compared with other ground features such as vegetation, crop lands, bare soil, urban area etc., shoreline is considered as a highly dynamic in nature and it needs to be continually monitored (Bouchahma and Yan 2012; Chand and Acharya 2010; Fenster, Dolan, and Morton 2001) because it is always influenced by wave actions, tidal variations, natural hazards, and anthropogenic impacts (Niya et al. 2013). Shoreline change is a function of erosion and accretion of the beach which is nourished with

materials by rivers, coral reefs and in some cases by erosion of shore fronts. When the average long-term supply of materials to the area considered is lower than the material moving out of the area, the coastal erosion occurs (Dayananda 1992). It is defined the shoreline as land-water boundary (Dolan, Fenster, and Holme 1991; Pajak and Leatherman 2002) and the position of the land-water boundary at one instant in time is known as the “instantaneous shoreline” (Gens 2010). In some cases wet-dry or vegetation line is used as a reference line to estimate the coastal changes (Boak and Turner 2005). Practically it is difficult to evaluate the shoreline changes within a short period of time. Long-term changes can be detected by carrying out comprehensive field surveys for a long period. Continuous ground monitoring is needed in this regard. But this is a labor intensive, expensive and time-consuming process (Daniels 2012; Liu, Sherman, and Gu 2007; Natesan et al. 2013; Warnasuriya 2015; Warnasuriya, Pradeep Kumara, and Alahacoon 2015). However, satellite remote sensing is one of the best solutions in order to investigate the shoreline change over a long period of time as it is cost effective and availability of temporal data at same locations of the ground (Chenthamilselvan, Kankara, and Rajan 2014; Geeganage and Warnasuriya 2016). Currently, the usage of satellite images is very popular among the researchers in the various disciplines for mapping of spatial and temporal ground variations (Bertacchini and Capra 2010; Lee and Jurkevich 1990; Lipakis, Chrysoulakis, and Kamarianakis 2005; Muthukumarasamy et al. 2013; Sankar et al. 2014; Warnasuriya 2015; White and El Asmar 1999). This helps to get a synoptic idea about the dynamic nature of the ground features in a vast area at a certain time (Mahapatra, Ratheesh, and Rajawat 2014).

Resolution of the satellite images is the main constraint for mapping which governs the accuracy and precision (Gens 2010). But this depends on the type of features, extend and the purpose of the study which is under investigation. Some studies such as mapping of land-use types which have low rate of changing nature with large extent (Lands, paddy fields, forests, water bodies, deserts etc.), can be satisfied with the satellite images bearing medium-resolution while high-resolution satellite images are highly needed to explain some highly sensitive phenomena to be explained (Appeaning Addo, Jayson-Quashigah, and Kufogbe 2012; Dewidar and Frihy 2010; Geeganage and Warnasuriya 2016; Murray et al. 2012; Quashigah, Addo, and Kodzo 2013). On the other hand, medium spatial resolution satellite images such as Landsat or Sentinel can be very effective in the case of provincial, national or global scale temporal mapping processes because these images are available with high temporal resolution for free of charge. As the shoreline has a highly dynamic and complex nature, it is better to use high-resolution satellite images for better results under large scale for the

ground area. Although aerial photographs and Light Detection and Ranging (LiDAR) technology provide high-resolution images, they are expensive and time-consuming process when covering a large area of the ground and thereof repeatability is difficult (Guariglia et al. 2006; Liu, Sherman, and Gu 2007; Morton, Miller, and Moore 2005; White and Wang 2003; Zhao et al. 2008). The accuracy of the shoreline change rate also depends on several factors such as the accuracy of the delineated shorelines, temporal resolution of the shoreline, number of shoreline positions considered to calculate the change rate, the proximity of each observation to the time of an actual change in the trend of shoreline movement, the period of time between the shoreline measurements, the total time span of shoreline data, and the method used to calculate the rate (Dolan, Fenster, and Holme 1991). Although the high-resolution images are available from various satellites with Digital Number (DN) values which give the sense of the reflectance, they are bit expensive. Comparative to that, the high-resolution satellite images from Google Earth (GE) platform are freely available, hence it is cost effective. Therefore, they can be effectively utilized for shoreline change mapping after the appropriate corrections.

A very few scientific studies have utilized the GE satellite images in mapping of temporal changes in coastal and marine ecosystems since these images do not store the reflectance in the form of DN or pixel values. Therefore, pixel-based image classifications and applying algorithms are not possible with these images. However, this can be used effectively for land-use mapping (Malarvizhi, Kumar, and Porchelvan 2016) and shoreline change mapping as these processes do not directly depend on pixel values. The boundaries of the land-use types can be easily demarcated by digitizing process which comes under the Geographic Information System (GIS) technology (Reddy 2008). Major advantages of using GE satellite images are availability of both medium to high resolution images and the availability of time series data (Malarvizhi, Kumar, and Porchelvan 2016). The resolutions are ranging from 30 m (Landsat) to 0.31 m (Worldview -3/4) and data are available from 2002 to date (Google Earth Pro 2017).

Major factors affecting for shoreline change are beach morphology, grain size of the beach sand, tide, waves, coastal water currents, wind, sea level rise, adjacent land-use types etc. (Cooper et al. 2004; Forbes et al. 2004; Lin and Pussella 2017; Orford, Forbes, and Jennings 2002). Both natural and anthropogenic impacts (Chen et al. 2005; Mujabar and Chandrasekar 2013; Sesli et al. 2009) enhance the shoreline change and alter the adjacent coastal habitats. Consequently, they influence accretion and coastal erosion. Here erosion means backward moment of the shoreline where accretion refers to forward moment of the shoreline (Nandi et al. 2016). Coastal communities are greatly affected in this circumstance. Therefore conducting

regular monitoring (Shalaby and Tateishi 2007) and hazard analysis of coastal environment is very important to ensure the environmental, social and economic vulnerabilities in the coastal nations.

For identification of vulnerable areas and applying the coastal management strategies, shoreline change analysis is an effective process (Lin and Pussella 2017; Makota, Sallema, and Mahika 2004) for the sustainable development of coastal environment by covering various aspects such as environmental, economic, and social. Generally the shoreline change can be estimated by measuring the differences between shoreline positions over a time period and changing rate is the distance of change per year (Dolan, Fenster, and Holme 1991).

This study was conducted in some selected coastal regions of Jaffna peninsula in Sri Lanka. These locations were selected mainly because, there are lots of socio-economic activities are taken place. Also, in the aspect of environment, these areas are very significant. Other main reason is there are lack of scientific studies carried out in the area due to the civil war period prevailed since 1980s to the latter part of the last decade. Accessibility to the regions is still problematic because the hazardous remnants of the war may still present all over the ground. Due to those reasons, this study will be helpful to encourage the discovering of scientific knowledge in these hidden parts of the world.

Therefore the main aim of this study is to develop an appropriate method to evaluate the shoreline change using remote sensing technology combining with GIS which is an effective tool for spatial and temporal planning (Green et al. 2000; Reddy 2008; Van and Binh 2009) and subsequently provide information for coastal resource management practices for decision making process with high accuracy levels. Besides, a very few studies have been carried out in Sri Lanka to estimate the shoreline change using high-resolution satellite images and most of the shoreline change studies were based on conventional aerial photographs, field data, and low-resolution data (Dayananda 1992; Geeganage and Warnasuriya 2016; Gunasekara and Alahacoon 2011; Weerakkody 1995).

Study area

The study was carried out along the north-east shoreline of Jaffna district in Sri Lanka. The study area lies between latitudes $9^{\circ} 49' 36''\text{N}$ to $9^{\circ} 35' 4''\text{N}$ and longitudes $80^{\circ} 15' 1''\text{E}$ to $80^{\circ} 27' 45''\text{E}$ (Figure 1). The average extent of the shoreline is 45 km starting from Point Pedro fisheries harbor to Pokkaruppu. The adjacent beach is sandy (fine to very fine sand) and flat with an almost straight shoreline. This belongs to the Point Pedro and Maruthkerny DS (Divisional Secretariat) Divisions and nineteen GN

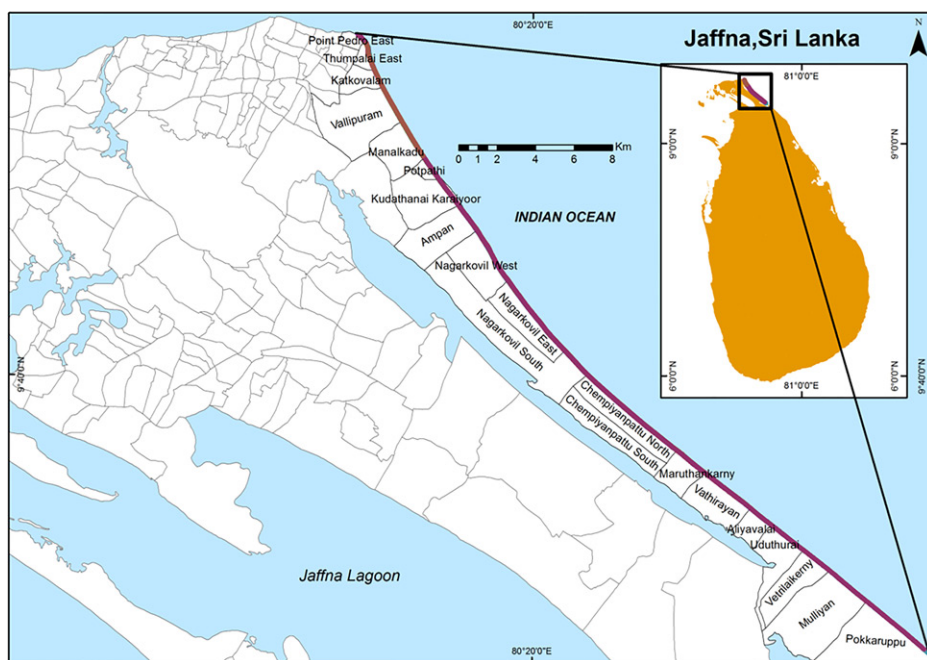


Figure 1. Location of the study area along the north-east shoreline of Jaffna district, Sri Lanka.

(Grama Niladari) divisions namely, Point Pedro East, Thumpalai East, Katkoyalam, Vallipuram, Manal kadu, Potpathi, Kudathanai Karaiyoor, Ampan, Nagarkovil West, Nagarkovil East, Nagarkovil South, Chempianpattu North, Maruthankarny, Vathirayan, Aliyavali, and Uduthurai, Vetrilaikerny, Mullian, Pokkaruppu (Survey Department of Sri Lanka 2007). Population of the above GN Divisions is ~ 21297 (Department of Census and Statistics 2008). Geological formation of the area comprises Miocene limestone (Abeyasinghe, n.d.; Geological Survey Department, and Department of Mines and Energy South Australia 1982). This is the main source for ground water store in Jaffna peninsula (Gunaalan et al. 2013). The major coastal ecosystem located in this area is sand dunes with coastal vegetation. Fishing is the main socio-economic activity of this coastal region while the agriculture and animal husbandry contribute to a certain extent. The area falls within the dry zone of the county and the annual average temperature recorded in 2015 was 28.18°C while the annual average rainfall was 1838.9 mm (District Secretariat Jaffna 2016). The area is influenced by the rainfall during the second inter-monsoon period (October to November) and north-east monsoon period (December to February) (Department of Meteorology Sri Lanka 2016). Tide is usually diurnal and the Mean High Water Spring (MHWS) is about 0.7 m while the Mean High Water Neap (MHWN) is about 0.5 m. Mean Low Water Neap (MLWN) and Mean Low Water Spring (MLWS) are 0.2 and 0.1 m respectively (Morris 1987). Surface currents towards the east of

the north-east coast are very strong during the north-east monsoon. According to the Sri Lankan coastal wave climate, the area belongs to the Low Energy Zone which is having 0.4–2.0 m wave height in the south-west monsoon period while 1.5–2.7 m wave height in north-east monsoon period. The wave height during inter-monsoon periods lies between 0.4 m and 1.5 m (Survey Department of Sri Lanka 2007). Some of the shorelines in the area are highly influenced by seasonal variations (Gunasekara and Alahacoon 2011).

Methodology

GE high resolution satellite images were used to extract the instantaneous shorelines for the years 2002, 2003, 2006, 2009, 2011, 2013, 2014, 2016, and 2017 covering a period of 15 years. In 2002 and 2009, there were two satellite images for two different months and in 2011 there were five satellite images for five different months. These images were used to estimate the seasonal variation of shorelines. Approximate spatial resolution of the images lies between 0.31 and 2 m and it is shown in Table 1 (Astrium 2017; Digital Globe 2017). Land-Water boundary was considered as the shoreline in this study and the blue margin which separates the land from water in the images was used as reference line through visual interpretation because the wave action in the area is comparatively low. Ground survey was carried out three times during the period of 2015–2017 in order to obtain Ground Control Points (GCPs) in the places such as shoreline positions, beach slopes, permanent structures (pillars, houses, harbors etc.), adjacent ecosystems (sand dunes, vegetation, water bodies etc.) and in the places which reflect the beach status (erosion or accretion). GCP locations

Table 1. Image source and approximate spatial resolution of the high-resolution satellite images from Google Earth platform.

Date of acquisition	Image source	Approximate spatial resolution (m)
1/12/2002	Digital Globe	0.65–1.00
5/24/2002	Digital Globe	0.65–1.00
3/24/2003	Digital Globe	0.65–1.00
5/17/2006	Digital Globe	0.65–1.00
6/4/2009	Digital Globe	0.5–1.84
9/11/2009	Digital Globe	0.5–1.84
2/17/2011	Digital Globe	0.5–1.85
3/8/2011	Digital Globe	0.5–1.85
7/7/2011	Digital Globe	0.5–1.85
9/8/2011	Digital Globe	0.5–1.85
12/4/2011	Digital Globe	0.5–1.85
4/27/2013	Digital Globe	0.5–1.85
2/9/2014	CNES/Astrium	0.5–2.00
4/7/2016	Digital Globe	0.31–1.85
1/9/2017	CNES/Astrium	0.5–2.00

Note: Approximate spatial resolution was determined by referring to the data source and by visual interpretation of each GE image by examining the minimum possible object which could be observed.

were obtained during the ground survey using the handheld Magellan eXplorist 610 GPS (Global positioning system) machine which has the 4 m accuracy. Other information sources used in this study are community interviews, published reports, nautical charts, topographic maps, and other relevant literature. Overall idea about the current and past nature of the coastal environment was identified by the personal views of the community via community interviews. Published reports were used to get an overall idea about the land-use types, demography, geography, climate of the study area and so on. Nautical charts were used to find the tide level of the coastal region. Topographic maps and other literature were used to identify the different features of the ground with respect to the GN Divisions. All these information was used as a guide for the accuracy assessment. Wave climate was analyzed by plotting wave rose for each month using ERA-interim data for the period from Jan 2000 to Dec 2016 at an offshore location (80.50E, 9.75N). Wave rose was plotted by using MATLAB 2017a software.

Shoreline extraction from GE software (version 7.1.2.2041 and 7.3.0.3832)

Before extracting the shorelines, the tilt of the images of the study area was adjusted in the GE software in order to minimize the geometric distortions and the scale was kept similar for each image throughout the digitizing process. Then shorelines were delineated for the aforementioned years based on the satellite images from GE platform (same eye altitude (500 m) was adjusted for all satellite images to remove the error causing during the digitizing process due to zoom level) in the GE software itself. These shorelines were saved in KML (Keyhole Markup Language) file format. Subsequently, the KML shoreline files were converted to the “Layer files” from ArcGIS 10.4.1 software. All shorelines extracted from GE were overlaid and managed in a personal geodatabase in ArcGIS 10.4.1 software. Accuracy of the satellite images was checked using 40 GCPs and geometric corrections were applied to each shoreline before the analyzing process. GCPs are shown in the [Figure 2](#).

Accuracy test for shoreline rectification

Slight shifts of the GE satellite images due to the georeferencing errors, platform-oriented errors and errors due to the zenith angle were estimated with reference to the GCPs in the image (2013) which is closely related to the ground truth data. Permanent structures such as tips of roofs of square buildings were used as GCPs in this regard and these structures were represented in all the satellite images considered in this study. Tips of the roofs were taken into account because the position of these tips does not vary

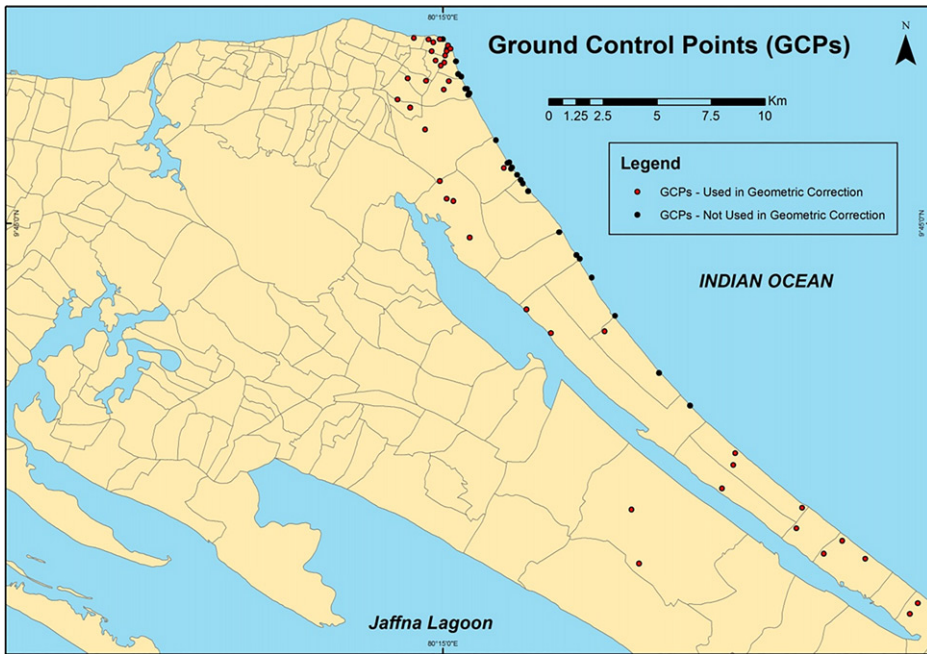


Figure 2. Ground control points used in the study.

due to the zenith angle and the altitude of the satellite at the time of image acquisition. GCPs of shoreline positions could not be used for the ground truthing of the shoreline as the survey was not performed at the time of satellite overpass. However, the shoreline positions and some other GCPs obtained during the ground survey were used as a reference guide to get an overall idea about the study area and to select the image which is closely related to ground truth data.

Standard deviation (SD) of the positional shift was used as one of the uncertainties (U1) for shoreline change detection using DSAS tool bar (extension) in ArcGIS software. The digitizing of the same shoreline was done twice in GE software itself in two different times under same conditions in order to estimate the digitizing error (Note that shoreline change statistics were calculated based on initially digitized shoreline). Both first and second shorelines delineated in GE software were saved in KML file format. After adding both shorelines into the ArcGIS platform, they were converted into shape files (layer files) which are compatible for further analysis in GIS platform. The deviation of the same shoreline in the digitizing process under the aforementioned two different scenarios was calculated in DSAS in ArcGIS 10.4.1 software. Mean SCE was calculated for these two shorelines which represent same area of the ground and it was used as the mean deviation. This value is considered as the digitizing error of the shoreline in this study. This method was applied to all other shorelines to calculate the respective digitizing error in each shoreline. Outliers were

identified by producing boxplots in SPSS 16.0 and R 3.2.1 statistical software (Outliers were plotted as individual points) and eliminated those values from the data sets in order to minimize the errors introduced in the calculation of digitizing error in each shoreline because slip of the hand may cause significant errors in digitizing. This is also incorporated to the uncertainty value (U2). Due to the tide, the shoreline can be changed. Therefore, the tidal error is also added to calculate the uncertainty (U3). The average spring tide variation in north-east coastal waters of Sri Lanka is 0.6 m while the average neap tide variation is 0.2 m (Morris, 1987). Based on this, the influence on the shoreline due to the tide was calculated using the following equation (Eq. 1).

$$\tan\theta = \frac{\text{Average tide variation (m)}}{\text{shoreline displacement (m)}} \quad (1)$$

where, θ = slope angle in degrees

The average slope of the beach was estimated using the standard survey techniques.

Cumulative uncertainty (U) was calculated for each shoreline using the following equation (Eq. 2) and used in DSAS (Digital Shoreline Analysis System) 4.3 tool bar (extension) in ArcGIS software in order to calculate shoreline change statistics.

$$U = U1 + U2 + U3 \quad (2)$$

where,

U1 = Uncertainty due to the positional shift of satellite image in meters.

U2 = Uncertainty due to the digitizing error in meters.

U3 = Uncertainty due to the tidal error in meters.

Data preprocessing

Based on the positional shifting of the satellite images (shifting of the image also concurrently shifts the shoreline), all the digitized shorelines were rectified geometrically in the ArcGIS software by considering both mean shift angle and mean shift distance using “Editor” tool which is used in digitizing process. They were subjected to WGS 84 Universal Transverse Mercator (UTM) projection (Zone 44N) and all the shoreline layers were managed in a personal geodatabase in ArcGIS 10.4.1 software.

Defining the best transect interval

A preliminary experiment was carried out to find the best transect interval to calculate change statistics of the shoreline under predefined five transect interval scenarios such as 5 m, 10 m, 25 m, 50 m, and 100 m. It was assumed

that the 5 m scenario has the highest accuracy as it reflects the most part of the shoreline compared to the other scenarios considered in the study. As the accuracy and the efficiency are key functions in this regard, an index was developed to define the best transect interval for this study. For that purpose, the shoreline change between 12/01/2002 and 24/05/2002 was calculated as a model by using DSAS tool in ArcGIS 10.4.1 and calculated the time duration taken for the data processing for shoreline change analysis under each transect interval scenario. Subsequently, independent sample *t*-test was executed for the shoreline change values between different scenarios with respect to 5 m scenario using SPSS 16.0 and R 3.2.1 software and significant values of Levene's Test for Equality of Variances which describe the variability (same or different) between two scenarios were obtained as the results of the *t*-test showed that there is no significant difference ($P > 0.05$) in the means between two scenarios. If the significant value of Levene's Test for Equality of Variances is greater than 0.05, it means that the variability in the two scenarios is not significantly different. Based on those parameters, the following index was devolved to select the best transect interval for the study and this index was named as Shoreline Change Analysis Transect Interval Index (SCATI). According to the index value, the highest value indicates the more suitability for the selection of transect interval. Speed of the computer remained same at each scenario.

$$\text{SCATI} = P/T$$

where,

P = Significant values of Levene's Test for Equality of Variances.

T = Time taken for the data processing in minutes.

Data processing for shoreline change statistical analysis

Date field and uncertainty field were added to each shoreline layer and data were entered to the respective attribute tables. All the shoreline layers were appended to a single shapefile in a single geodatabase. A baseline was created on landward side with reference to all the digitized shorelines. Transect layer was created by casting transects in 25 m intervals along the baseline allowing to cross all the shorelines and 1767 transects were represented the entire study area. Transect length was set to 100 m.

Data analysis

Shoreline change analysis using DSAS

Shoreline change statistics for Net Shoreline Movement (NSM), End Point Rate (EPR), Shoreline Change Envelop (SCE) and Weighted Linear Regression Rate (WLR) were calculated to estimate the shoreline change during the study period by using of DSAS 4.3 tool bar (extension) in

ArcGIS 10.4.1 software. Net Shoreline Movement gives the distance between the oldest and youngest shorelines for each transect. Dolan, Fenster, and Holme (1991) explained that the EPR is the distance between two shoreline positions (earliest and latest) divided by the time elapsed between the measurements (Eq. 3). Average of Rates (AOR) method developed by Froster and Savage in 1989 (Genz et al. 2007; Thieler, O'Connell, and Schupp 2001) for calculating the shoreline change rate (Eq. 4) was used in the shoreline change rate analysis when the seasons of the available shorelines were taken into consideration. This approach was used to predict future changes based on the most recent trend of shoreline change. Shoreline change dynamism was estimated by using the Eq. 5.

$$\text{EPR} = D/T \quad (3)$$

where,

D = Distance between two shorelines in meters.

T = Time difference in years.

$$\text{AOR} = \text{EPR}_1 + \text{EPR}_2 + \text{EPR}_3 + \dots \text{EPR}_i/N \quad (4)$$

where,

N = Number of shorelines.

$$\text{Shoreline dynamism} = \text{SCE}/T \quad (5)$$

where,

T = Time difference in years.

SCE explains the distance between farthest and closest shoreline to the baseline at each transect and the results were used to explain the shoreline dynamism. In order to calculate the best-fit line in conjunction with uncertainty values, WLR was applied and under this, more reliable data are given greater emphasis or weight towards determining a best fit line (Himmelstoss 2009). Supplemental statistics such as Standard Error of Weighted Linear Regression (WSE), R-Squared value of Weighted Linear Regression (WR2) and Confidence Interval (95%) of Weighted Linear Regression (WCI) were used with WLR to ensure the accuracy and reliability of the estimate. In addition, Confidence of End Point Rate (ECI) was used to support the interpretation of EPR.

Shoreline change statistics were calculated to understand the overall change, inter-seasonal change during a year and intra-seasonal change among years. Overall change was based on all the available shorelines without considering the seasonal influences and other two were calculated by considering the seasonal influences.

Statistical analysis for correlation

Pearson correlation coefficient was calculated using R 3.2.1 software to find the correlations of selected shorelines where the highest regression and

lowest regression values performed from the DSAS analysis between WLR and the time (year) (Figure 3).

Results and discussions

Although there are 15 shorelines were considered for covering the period of 15 years, all the shorelines cannot be used simultaneously to estimate the shoreline change due to two reasons. One reason is the shoreline gaps which do not represent the total length of shoreline considered in this study (as shown in Figure 5). But even small part of the shoreline is very important in the case of estimating the shoreline change trend over the study period. Therefore, short shorelines with gaps were used to understand the current shoreline dynamic trend and subsequently, it was used for the future prediction. The other reason is all the shorelines do not reflect the shoreline position restricted to one particular climate season of the country. Based on the month of each shoreline, they were categorized into three seasons such as north-east, south-west and first inter-monsoon

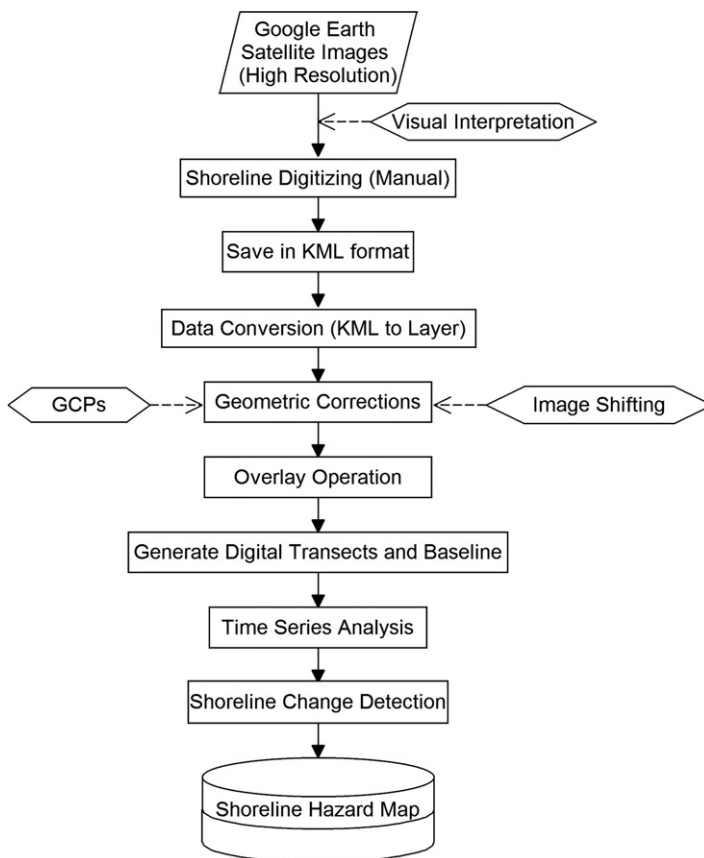


Figure 3. Flow chart of the methodology.

respectively (Table 2). Therefore, these shorelines representing for each season were used to estimate the both annual and seasonal shoreline change separately. Since the shoreline is subjected to change in season wise in a considerable way, it is better not to use shorelines from different seasons to estimate the annual variations. But shorelines from different seasons are ideal to use to estimate the seasonal variation.

According to the calculated shoreline length given in the Table 2, the longest shoreline was in 2017 and it covers the total study area while the shortest shoreline was recorded in 2011. All other shorelines themselves do not cover the whole stretch of the study area as the GE provides only certain regions. On the other hand, all the available shorelines do not represent the same season of the year. Five of them represent north-east monsoon and six of them represent south-west monsoon. There are four shorelines which represent first inter monsoon period of the country. As five shorelines were available in 2011, it is an essential component in order to estimate the seasonal variation taken place in a year. In addition to that, two shorelines were available for the years 2002 and 2006. Both shorelines in 2009 represent south-west monsoon thereof it is possible to calculate any significant change in shoreline within same season in the same year. Furthermore, there are two shorelines in 2011 represent north-east monsoon (17 February 2011 and 4 December 2011) and another two shorelines in 2011 represent south-west monsoon (7 July 2011 and 8 September 2011). The maximum available shoreline length for the study period was in 9 January 2017 (45.1 km) while the minimum shoreline length was recorded in 7 July 2011 (6.7 km). Figure 4 shows some part of the resulting map of the overlaid shorelines, baseline and transect with respect to GN Divisions, while the Figure 5 illustrates the length and gap of all digitized shorelines and their positions with regard to GN Divisions.

Table 2. Monsoon period, shoreline length and coordinates of each shoreline.

Date	Monsoon period	Shoreline length (km)	Coordinates (Start)		Coordinates (End)	
			Lat (N)	Long (E)	Lat (N)	Long (E)
1/12/2002	Northeast	16.25	9°49'36.478"N	80°15'0.691"E	9°42'17.096"N	80°19'34.908"E
5/24/2002	Southwest	11.52	9°49'36.981"N	80°15'0.232"E	9°44'26.7"N	80°18'9.82"E
3/24/2003	First inter	25.55	9°45'8.679"N	80°17'37.156"E	9°35'33.541"N	80°27'5.992"E
5/17/2006	Southwest	24.50	9°44'16.279"N	80°18'17.553"E	9°35'7.053"N	80°27'40.915"E
6/4/2009	Southwest	20.46	9°45'46.422"N	80°17'9.375"E	9°37'37.915"N	80°24'26.464"E
9/11/2009	Southwest	14.16	9°49'36.344"N	80°15'1.375"E	9°43'19.219"N	80°18'52.994"E
2/17/2011	Northeast	21.62	9°44'33.655"N	80°18'3.982"E	9°36'27.303"N	80°25'58.265"E
3/8/2011	First inter	25.33	9°44'41.479"N	80°17'57.933"E	9°35'11.735"N	80°27'34.655"E
7/7/2011	Southwest	6.70	9°49'21.715"N	80°15'14.718"E	9°46'11.688"N	80°16'51.972"E
9/8/2011	Southwest	22.02	9°44'22.535"N	80°18'12.942"E	9°36'2.867"N	80°26'28.834"E
12/4/2011	Northeast	19.63	9°49'36.445"N	80°15'1.496"E	9°40'58.21"N	80°20'40.022"E
4/27/2013	First inter	21.36	9°49'36.453"N	80°15'1.544"E	9°40'11.819"N	80°21'23.41"E
2/9/2014	Northeast	31.75	9°42'17.45"N	80°19'35.196"E	9°31'27.073"N	80°32'7.817"E
4/7/2016	First inter	28.72	9°47'57.472"N	80°15'49.02"E	9°36'29.308"N	80°25'55.651"E
1/9/2017	Northeast	45.10	9°49'36.555"N	80°15'1.547"E	9°32'16.743"N	80°31'10.298"E

"Lat" refers Latitude while "Long" refers Longitude.

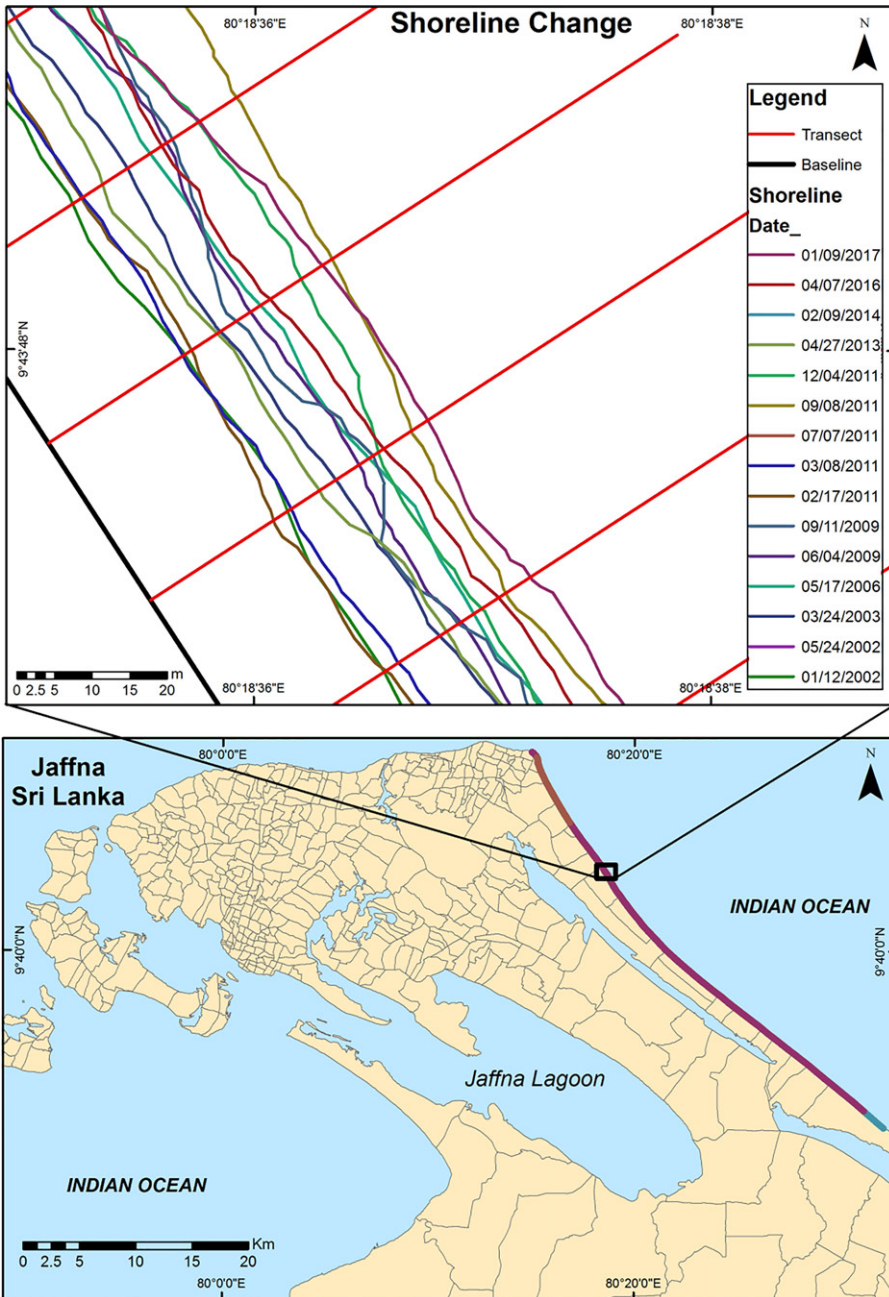


Figure 4. Resulting shorelines, baseline and transects.

According to the [Figure 5](#) it depicts that the Nagarkovil West and part of Ampan GN Divisions have the highest number of shoreline intersections (12 shorelines) while Vetrilaikerny, Mulliyan, and Pokkaruppu GN Divisions have the lowest number of shoreline intersections (2 shorelines). Other all GN Divisions have intersected more than seven shorelines other

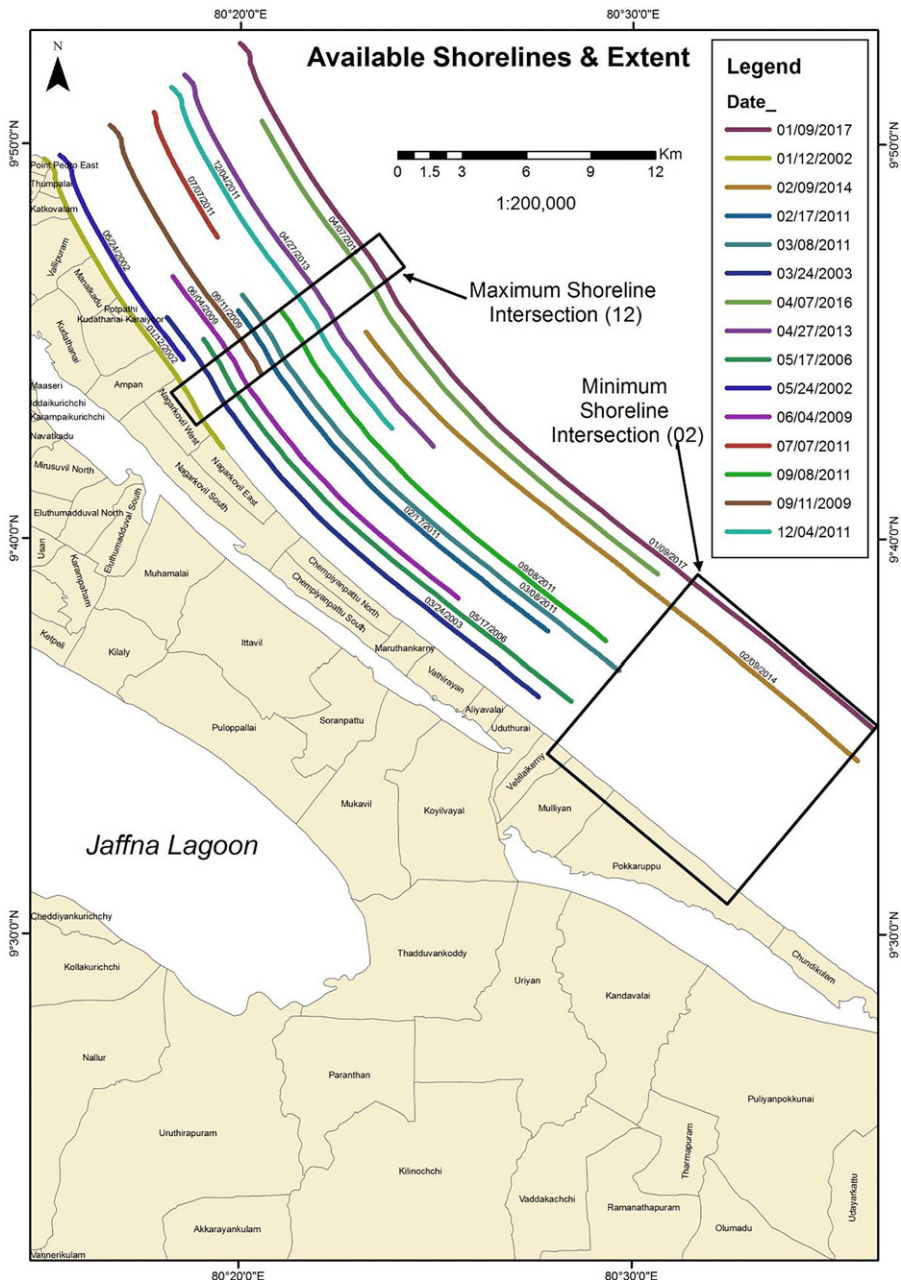


Figure 5. Diagrammatic representation of the relative position of the shorelines relevant to Grama Niladari Divisions.

than Aliyavalai, Uduthurai DN Divisions. **Figure 6** shows the percentage values of the shoreline length based on the minimum threshold values of the shoreline intersection.

According to the **Figure 6**, entire shoreline of the study area pertains more than two shorelines while the 71.11% of the shoreline pertains at least

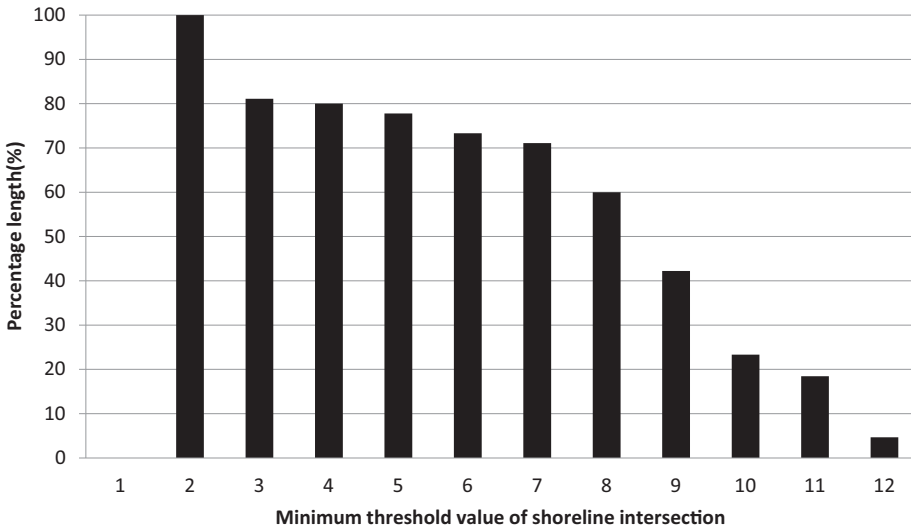


Figure 6. The graph of percentage values of the shoreline length against the minimum threshold values of the shoreline intersection.

Note: Minimum threshold value refers the minimum number of shorelines a transect must intersect in the analysis

7 shorelines in temporal scale. Only 4.67% of the shoreline covers the maximum number of shoreline intersection (12 shorelines). In order to calculate the shoreline change statistics using DSAS such as NSM, EPR, and SCE, there should at least 2 shorelines are to be intersected while at least 3 shorelines are needed to calculate WLR. Therefore, WLR cannot be calculated for the shorelines where only two shorelines are available (Vetrilaikerny, Mulliyan, and Pokkaruppu).

As the shoreline is a highly dynamic feature and its changes are taken place in short time spans, it is very important to gather shorelines very accurately in the temporal and spatial scales as much as possible. Because even the slight shift of the shoreline in terms of georeferencing or overlapping errors of the maps will introduce significant errors in the final results. For instance, shoreline parallel shift error between the shorelines delineated for two different time period will indicate the actual erosion areas as accretionary areas and vice versa. If it is so, it gives a completely wrong idea about the shoreline status over a particular time period. In order to avoid this problem, it is necessary to apply geometric corrections and calculate the uncertainty of the delineated shorelines. In this study the uncertainty was calculated based on three criteria namely, shoreline shifting error, digitizing error and tidal error. As the tidal change in the northern part of the country is very small (0.2–0.6 m), the impact on the shoreline change due to tide variation is also very small. The calculated uncertainty values for each delineated shorelines are given in the [Table 3](#).

Table 3. Uncertainty of shorelines.

Date	Shifting error/m	Digitizing error/m	Tide error/m	Uncertainty/m
1/12/2002	0.820737	1.024674	1.65	3.495411
5/24/2002	0.602941	1.035183	1.65	3.288124
3/24/2003	0.141926	1.402524	1.65	3.19445
5/17/2006	1.079249	2.534207	1.65	4.676345
6/4/2009	1.504031	0.949535	1.65	4.103566
9/11/2009	0.740704	1.012514	1.65	3.403218
2/17/2011	1.218038	1.202654	1.65	4.070692
3/8/2011	0.887778	1.311668	1.65	3.849446
7/7/2011	0.488197	0.863137	1.65	3.001334
9/8/2011	1.243316	1.266625	1.65	4.159941
12/4/2011	0.700312	1.028393	1.65	3.378705
4/27/2013	0	1.127405	1.65	2.777405
2/9/2014	0.739001	1.637261	1.65	4.026262
4/7/2016	0.770455	1.30932	1.65	3.729775
1/9/2017	1.054661	2.127237	1.65	4.831898

Mean uncertainty of the shoreline is 3.73 ± 0.59 m and therefore the accuracy of the study can be considered as high (Gens 2010). The uncertainty values were used in DSAS in order to calculate the WLR which gives the shoreline change trend over the study period and subsequently, this can be used to predict the future changes. Tidal error was calculated by using the slope angle of the swash zone (20°) with maximum tidal change (0.6 m) and it was assumed that the slope angle and the maximum tidal change have not changed during the study period. Therefore, tidal error remained constant throughout the study period with the value 1.65 m. This depends upon the time of the day that the satellite image is captured. Unfortunately, the time of the data acquisition is not available in GE satellite images.

During this study it was identified that the processing time for the analysis of the shoreline change statistics is getting higher with the increasing number of transects used in the calculations as it has to use more intersecting points in the processing process in DSAS. On the other hand, more transects mean more accuracy as it reflects the most part of the shoreline which is under investigation. Since the time is one of the key factors as far as the efficiency is concerned, it is very critical to identify the best transect interval in order to fulfill both accuracy and the efficiency results. This could be achieved by obtaining the ratio between significant values of Levene's Test for Equality of Variances and the processing time and this was named as SCATI index. Significant value of Levene's Test for Equality of Variances is proportional to the accuracy while the time is inversely proportional to the efficiency. According to the SCATI index, best transect interval was identified as 25 m (0.1877) out of the five scenarios considered to test this in the study. Five meter scenario was used as the control as this has the highest accuracy and all other scenarios were compared with the control by using independent sample *t*-test and it showed that there is no any significant difference in each scenario ($P > 0.05$). The SCATI index for each scenario is shown in the Table 4.

Table 4. SCATI index.

Transect-Interval/m	SCATI index
5 (control)	0.0752
10	0.1412
25	0.1877
50	0.1763
100	0.0933

The overall shoreline change statistics based on the delineated all 15 shorelines under Mean, Standard deviation (SD), Maximum value (Max), and Minimum value (Min) are given in the Table 5. Minimum threshold value for the shoreline intersection used in this calculation was 2.

Net Shoreline Movement (NSM) and End Point Rate (EPR) consider the most recent and the farthest shorelines in the statistical calculation. In order to get the overall idea about the status of the entire shoreline, the aforementioned statistics were calculated disregarding the years of recent and farthest shorelines as the entire shoreline does not cover the same recent and farthest shorelines. Result shows that there is net shoreline accretion of 6.13 ± 8.74 m with an annual rate of deposition of 0.5 m/year. The confidence of the EPR (ECI) is 0.74 ± 0.68 . Shoreline Change Envelop (SCE) describes maximum change of the shoreline during the study period hence it gives the idea about how dynamic the shoreline is at particular place. According to SCE it shows that the highly dynamic shorelines with the maximum of 67.34 m erosion from 11 September 2009 to 9 January 2017 was in Thumpalai East GN Division and least dynamic shorelines with the minimum of 0.03 m accretion from 9 February 2014 to 9 January 2017 was in Vetrilaikerny GN Division (Figure 7). In the computation of rate-of-change statistics for future prediction purposes the weighted linear regression is more reliable to determine the best-fit line hence it was used in this study to make future prediction of the shoreline. Average Weighted Linear Regression Rate (WLR) was 0.24 m/year with accretion trend. Standard error of the estimate (WSE), Standard error of the slope with 95% confidence interval (WCI) and R-squared values (WR2) are 1.56 ± 0.66 , 5.03 ± 26.94 , 0.18 ± 0.18 , respectively. Maximum WR2 (0.99) was given by Point Pedro East DN Division closed to the breakwater in the fisheries harbor (Figure 8(a)). Therefore, it consolidates that the coastal structures such as breakwaters can accumulate the beach sand and follows the continuous accretion adjacent to it. The accretion in this area is taken place in the rate of 1.51 m/year. There was no any regression exhibited in 9.4% of the entire shoreline (Figure 8(b)).

As the Figure 8(a) has high coefficient of determination (R^2) it shows the definite shoreline change pattern ($r=0.9$) while the Figure 8(b) has an indefinite pattern of the shoreline as its R^2 is low ($r=0.2$). Based on the highest (more than $0.7 R^2$ value) and lowest (R^2 is less than 0.2) R^2 values

Table 5. Summary of the shoreline change statistics.

Shoreline change statistics	Mean	SD	Max	Min
NSM	6.13	8.74	35.32	-21.74
EPR	0.50	1.27	7.32	-6.44
SCE	16.59	8.17	67.34	0.03
WLR	0.24	0.51	1.54	-1.86
WR2	0.18	0.18	0.99	0
WSE	1.56	0.66	7.35	0.04

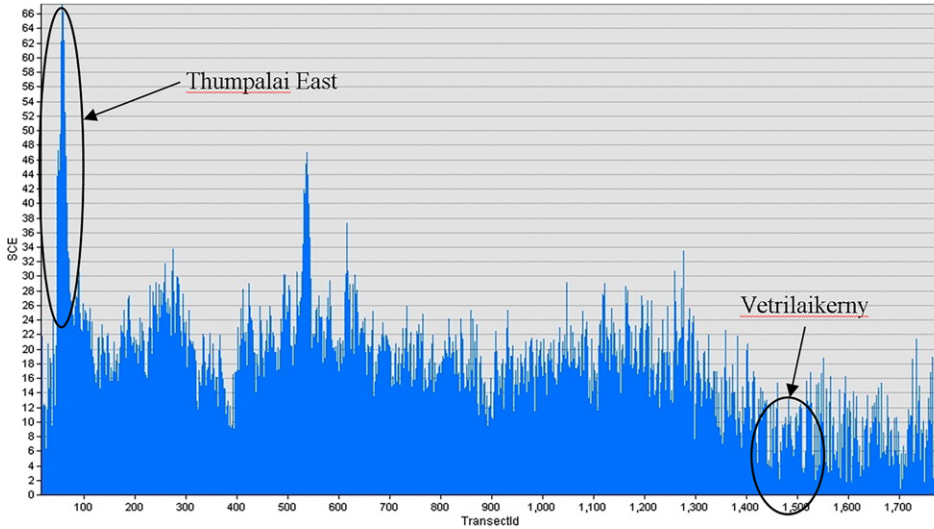


Figure 7. Shoreline change envelop along the shoreline at each transect.

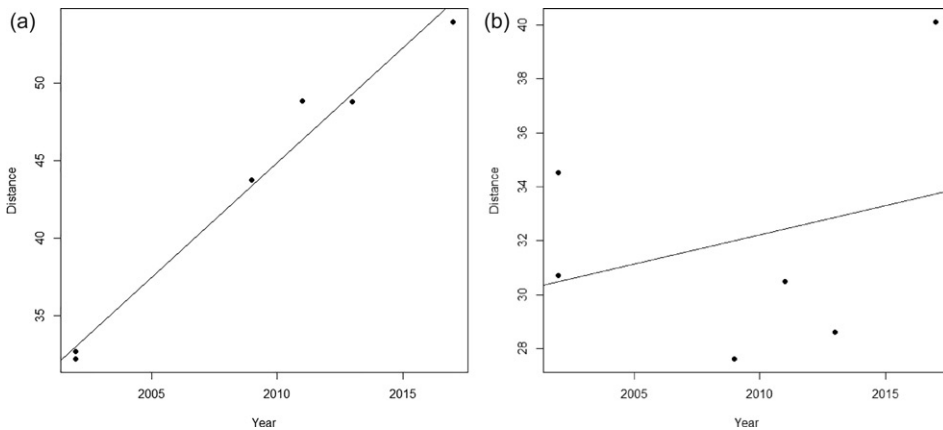


Figure 8. Highest (a) and Lowest (b) regressions based on shoreline positions from the baseline.

of the regression analysis, the predictable and unpredictable shorelines were mapped and they are shown in the Figures 9 and 10.

Highly predictable shorelines could be observed in some part of Point Pedro East, Thumpalai East, Manal kadu, Potpathi, Nagarkovil West, Aliavalai, and Uduthurai (Figure 9).



Figure 9. Highly predictable shorelines.

Highly unpredictable shorelines could be observed in some part of Point Pedro East, Katkovalam, Vallipuram, Potpathi, Kudathanai Karaiyoor, Ampan, Nagarkovil East, Nagarkovil South, Chempianputtu North, Maruthankarny, Vathirayan, Aliyavalai, and Uduthurai (Figure 10). Shoreline predictability and the unpredictability are very critical in Point Pedro East since there are lots of human activities are taken place (Figure 11).

According to the Figure 11, highly predicted accretions could be observed adjacent to the breakwater while the prediction for erosion is

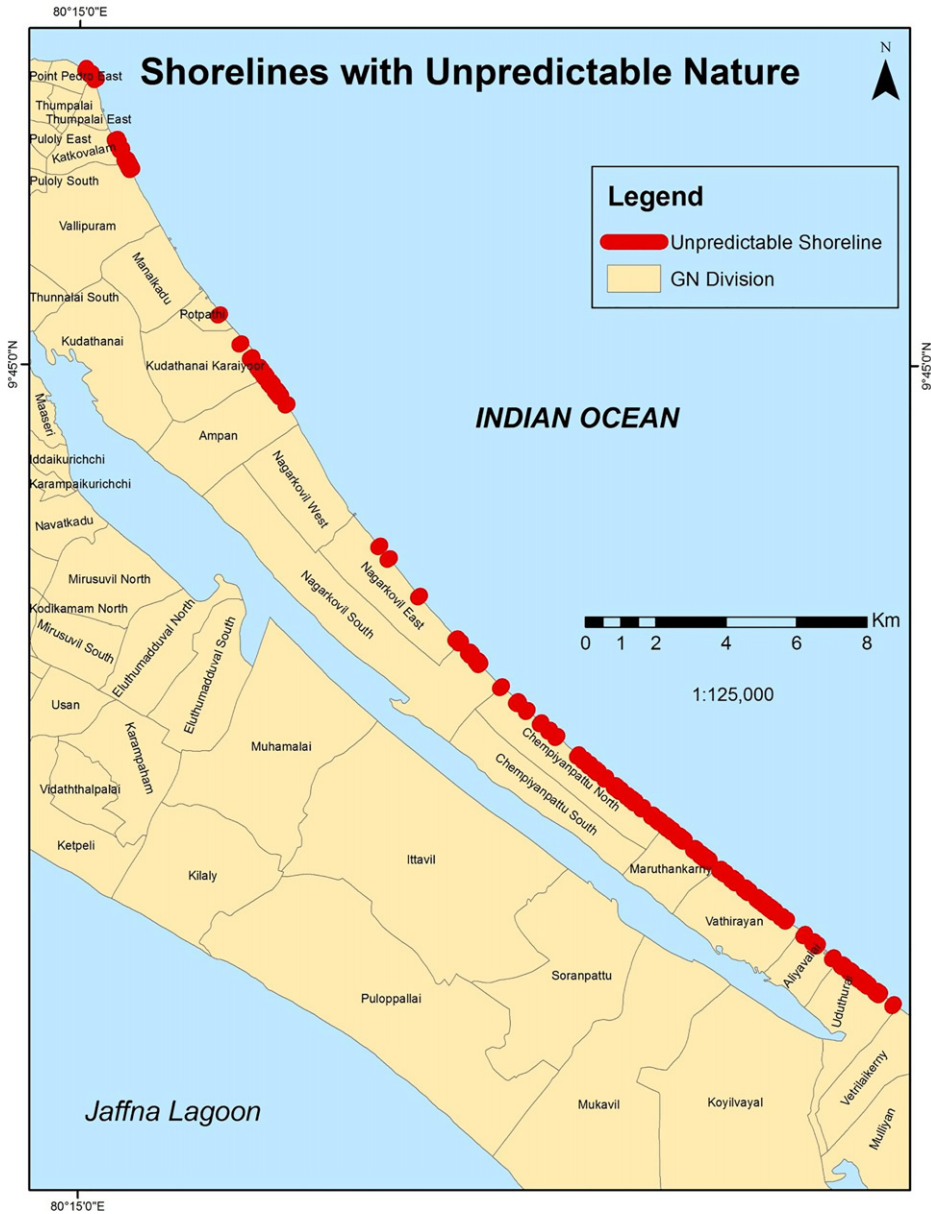


Figure 10. Highly unpredictable shoreline.

high at the end of the Point Pedro East GN Division. A few unpredictable zones also could be observed in this area.

During the study period, 76.12% of the observed shoreline is found accreted while the 23.88% of the shoreline is eroded (Figure 12). Shoreline status of each GN Division is given in the Table 6.

According to the Figure 13, it explains that most part of the shoreline in Point Pedro East is subjected to accrete rather than the erosion. Therefore, the shoreline in Point Pedro East is considered as a deposited shoreline.

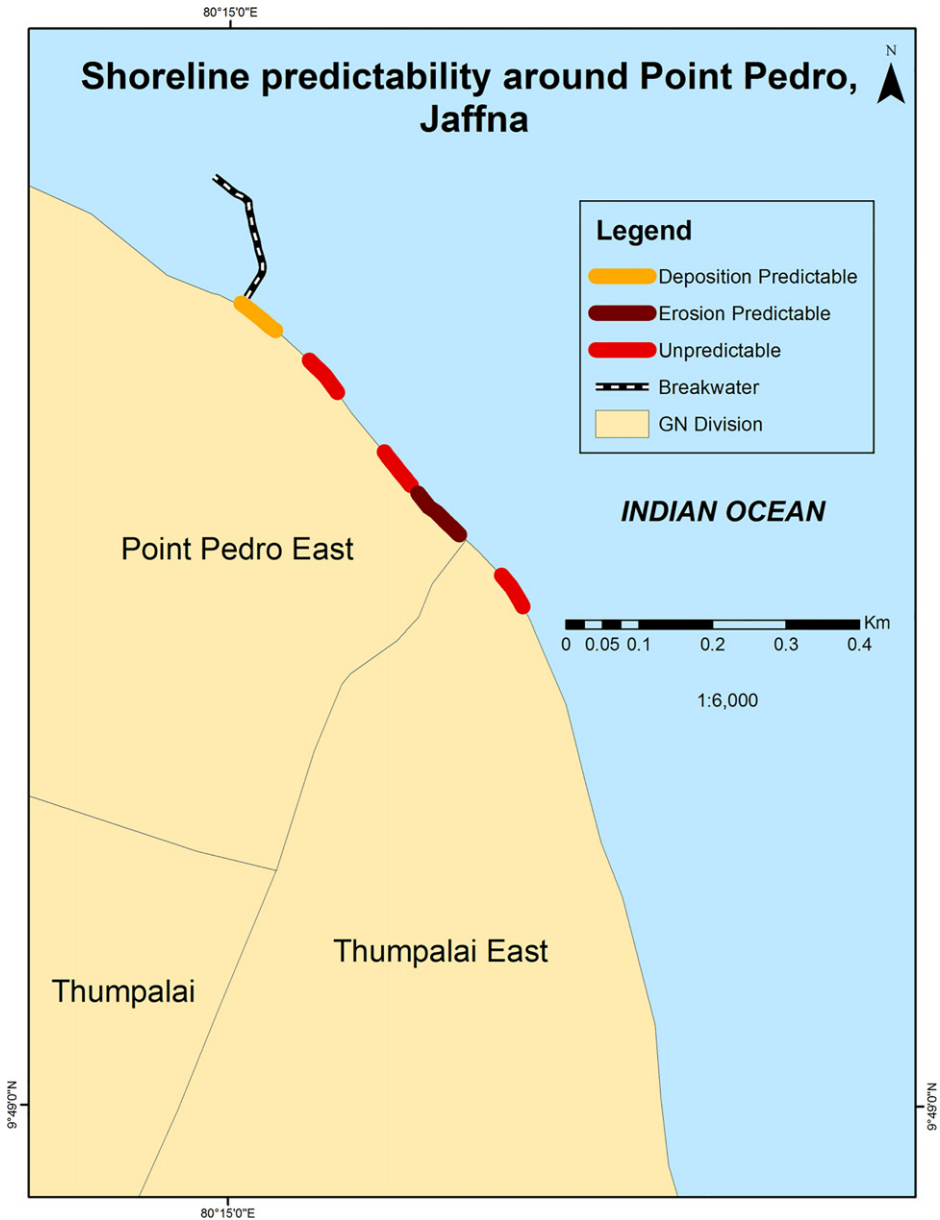


Figure 11. Shoreline predictability in the vicinity of Point Pedro East.

The reason for the accretion in this region is due to the construction of breakwater and it is followed by drastic erosion in the adjacent two DN Divisions namely Thumpalai East and Katkivalam. This is because the beach sand in those areas are transported towards the breakwater and deposited there. Therefore, the coastal structures laid by the humans are not always very effective in the sense of coastal protection as the accretion is taken place at one place while the erosion is taken place at another place along the shoreline. The coastal belt from Vallipuram to Chempiyanputtu

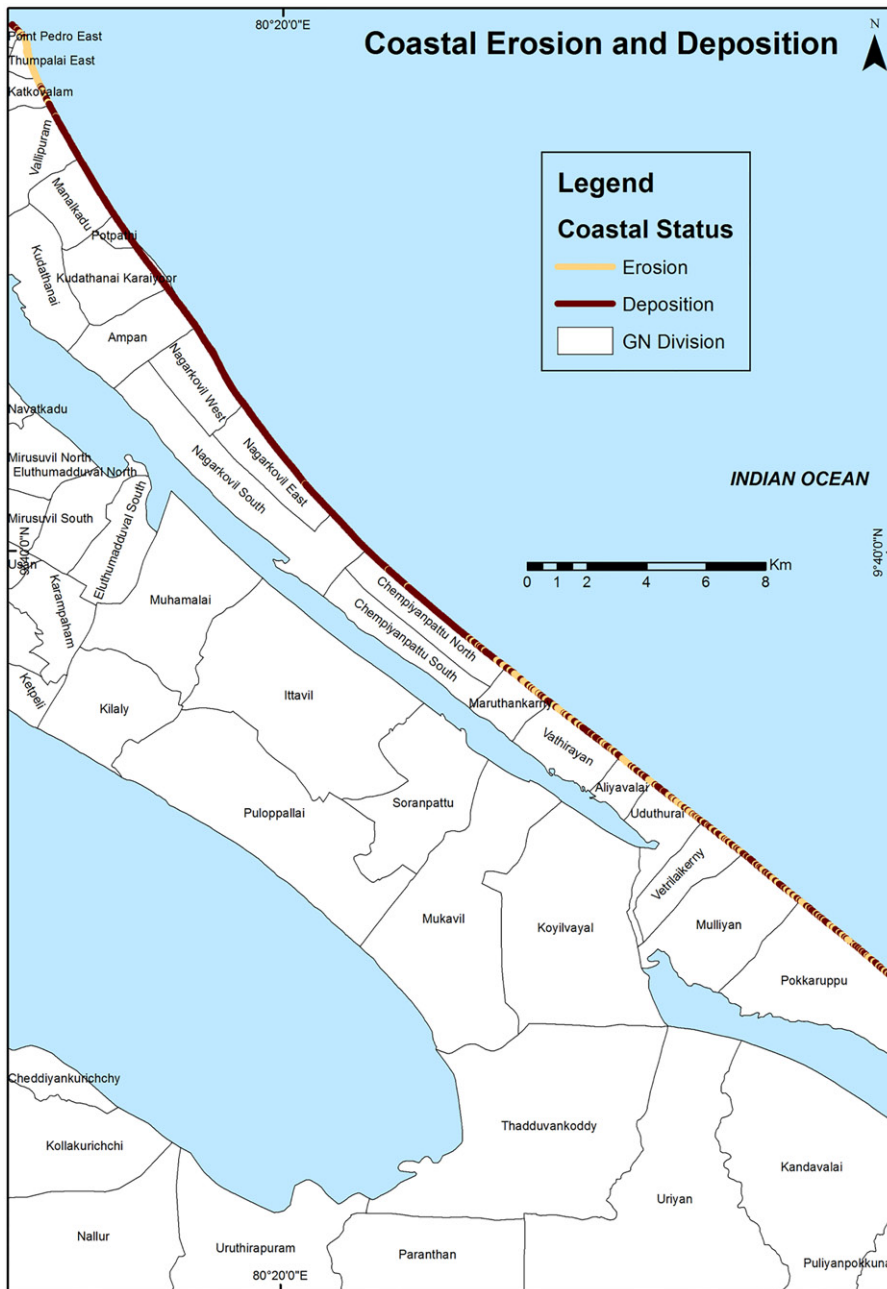


Figure 12. Shoreline hazard (erosion/accretion) map.

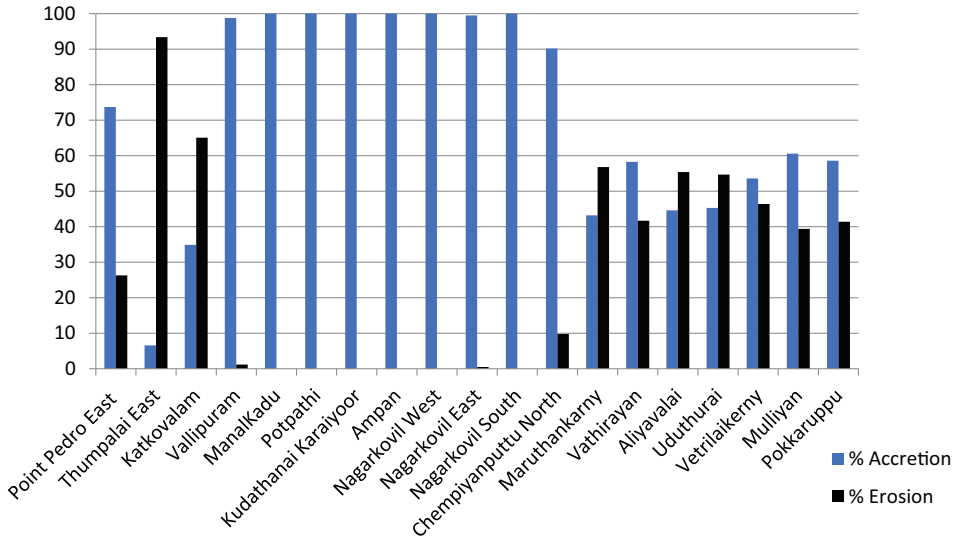
North has been subjected to almost 100% accretion. Other part of the shoreline has the alternate accretion and erosion pattern.

Mean shoreline change statistics for each GN Division are given in the Table 7.

The highest NSM is shown by Manal Kadu GN Division (18.62 ± 3.94 m) with accretion while the lowest NSM is shown by Vathirayan GN Division

Table 6. Shoreline status with GN divisions.

Coastal status	GN division	# GN divisions
Eroded area	Thumpalai East, Katkovalam,	2
Deposited area	Point Pedro East, Vallipuram, ManalKadu, Potpathi, Kudathanai Karaiyoor, Ampan, Nagarkovil West, Nagarkovil East, Nagarkovil South, Chempiyanputtu North,	10
Intermittent eroded-deposited area	Maruthankarny, Vathirayan, Aliyavalai, Uduthurai, Vetrilai kerny, Mulliy an, Pokkaruppu	7

**Figure 13.** Percentages of accretion and erosion among Grama Niladari divisions.**Table 7.** Mean shoreline change statistics in each Grama Niladari division.

GN division	NSM	EPR	SCE	WLR	WR2	WSE
Point Pedro East	3.81 ± 9.32	0.25 ± 0.62	13.44 ± 4.82	-0.06 ± 0.75	0.4 ± 0.35	0.99 ± 0.42
Thumpalai East	-7.98 ± 6.29	-0.53 ± 0.42	32.56 ± 15.85	-1.07 ± 0.4	0.34 ± 0.23	3.2 ± 1.92
Katkovalam	-2.42 ± 4.89	-0.16 ± 0.33	20.23 ± 3.72	-0.3 ± 0.21	0.07 ± 0.08	2.14 ± 0.32
Vallipuram	11.35 ± 4.63	0.76 ± 0.3	19.39 ± 3.3	0.48 ± 0.27	0.25 ± 0.17	1.62 ± 0.32
Manal Kadu	18.62 ± 3.94	1.24 ± 0.26	23.63 ± 4.01	0.94 ± 0.22	0.49 ± 0.12	1.64 ± 0.3
Potpathi	11.77 ± 3.81	0.79 ± 0.25	16.38 ± 3.13	0.43 ± 0.2	0.24 ± 0.18	1.45 ± 0.3
Kudathanai Karaiyoor	9.36 ± 3.4	0.62 ± 0.23	16.75 ± 5.49	0.24 ± 0.16	0.1 ± 0.1	1.54 ± 0.45
Ampan	9.91 ± 4.6	0.66 ± 0.3	20.25 ± 4.2	0.18 ± 0.37	0.08 ± 0.08	1.77 ± 0.26
Nagarkovil West	18.3 ± 5.87	1.22 ± 0.39	24.58 ± 7.04	0.8 ± 0.28	0.27 ± 0.1	1.79 ± 0.5
Nagarkovil East	10.22 ± 6.88	0.72 ± 0.45	18.83 ± 3.85	0.5 ± 0.26	0.19 ± 0.15	1.33 ± 0.26
Nagarkovil South	9.6 ± 4.69	0.7 ± 0.34	17.58 ± 3.66	0.29 ± 0.21	0.1 ± 0.13	1.29 ± 0.24
Chempiyanputtu north	6.14 ± 4.71	0.45 ± 0.34	16.81 ± 3.79	0.23 ± 0.25	0.1 ± 0.09	1.34 ± 0.28
Maruthankarny	-0.27 ± 4.7	-0.02 ± 0.34	19.65 ± 3.87	-0.15 ± 0.26	0.05 ± 0.07	1.62 ± 0.31
Vathirayan	0.22 ± 5.07	0.02 ± 0.37	17.85 ± 5.06	-0.05 ± 0.35	0.09 ± 0.12	1.53 ± 0.4
Aliyavalai	-0.62 ± 5.69	-0.05 ± 0.41	12.58 ± 4.17	-0.1 ± 0.47	0.24 ± 0.2	1.2 ± 0.37
Uduthurai	0.45 ± 4.55	0.1 ± 0.72	10.1 ± 4.68	-0.07 ± 0.36	0.16 ± 0.19	1.24 ± 0.59
Vetrilai kerny	0.89 ± 8	0.31 ± 2.74	6.94 ± 4	nil	nil	nil
Mulliy an	2.28 ± 7.97	0.78 ± 2.73	6.58 ± 5	nil	nil	nil
Pokkaruppu	1.39 ± 7.59	0.48 ± 2.61	6.34 ± 4.38	nil	nil	nil

(0.22 ± 5.07 m) with accretion. The highest EPR is also shown by Manal Kadu GN Division (1.24 ± 0.26 m/year) with accretion while the lowest EPR is shown by Vathirayan and Maruthankarny GN Divisions (0.02 ± 0.37 m/year and -0.02 ± 0.34 m/year, respectively). The highest SCE is shown by Thumpalai East (32.56 ± 15.85 m) while the lowest of it is shown by Pokkaruppu (6.34 ± 4.38 m) GN Division. The highest WLR is shown by Manal Kadu GN Division (0.94 ± 0.22 m/year) with accretion trend while the lowest WLR is shown by Vathirayan (-0.05 ± 0.35 m/year) with erosion trend. WLR could not be calculated for Vetrilaikerny, Mulliyan, and Pokkaruppu GN Divisions as only two shorelines were available. According to One-Way ANOVA, there is a significant difference of NSM, EPR, SCE, and WLR between GN Divisions ($P < 0.05$).

Since the shoreline change statistics such as linear regression analysis was influenced by the seasonal changes, the statistics were again calculated for same seasons in different years. Furthermore, seasonal change of the shoreline was estimated based on the shorelines in 2011 as it is the only year which has more than two shorelines representing three seasons of the year. Summary of the results are given in the Table 8. However, none of the years have shorelines from second inter-monsoon period.

According to the Table 8, inter-seasonal changes were estimated for the year 2011 and intra-seasonal changes were estimated for same season in different years under north-east, south-west, and first inter-monsoon periods. Mean EPR, SCE, NSM and WLR for the intra-seasonal changes are 0.9 ± 0.32 m/year, 9.84 ± 1.57 m, 5.25 ± 2.54 m, 0.75 ± 0.6 m/year, respectively. Mean R^2 value of the weighted linear regression is just above the 0.5 while the maximum of 0.7 ± 0.3 was recorded by the analysis for south-east monsoon. Mean standard error of the estimate is 1.12 ± 0.17 m. The problem of this calculation is entire study area is not covered due to the satellite data gaps and 72.27% of the study area is occupied by north-east monsoon while south-west monsoon occupies 60.33%. First inter-monsoon period was covered 70.46% of the study area in this calculation. The seasonal changes of the shoreline in 2011 from end of the north-east monsoon to end of the south-west monsoon under Mean EPR, SCE, NSM, and WLR are 1.31 ± 1.18 m/month, 13.24 ± 6.84 m, 9.3 ± 7.56 m, 1.81 ± 0.78 m/month, respectively. R^2 value of the weighted linear regression of this calculation is

Table 8. Inter-seasonal and intra-seasonal shoreline change.

Monsoon period	EPR	SCE	NSM	WLR	WR2	WSE
Northeast	0.98 ± 1.62	11.64 ± 6.45	7.77 ± 8.98	1.23 ± 0.95	0.7 ± 0.3	1.15 ± 0.84
Southwest	1.18 ± 2.6	9.17 ± 5.31	5.28 ± 7.77	0.94 ± 1.17	0.64 ± 0.33	0.93 ± 1.08
First-inter	0.55 ± 1.09	8.72 ± 4.54	2.69 ± 6.02	0.06 ± 0.41	0.34 ± 0.31	1.27 ± 0.67
All monsoons	1.31 ± 1.18	13.24 ± 6.84	9.3 ± 7.56	1.81 ± 0.78	0.8 ± 0.2	0.98 ± 0.67

Note: Values for all monsoons are from the year 2011. EPR and WLR under this were calculated per month.

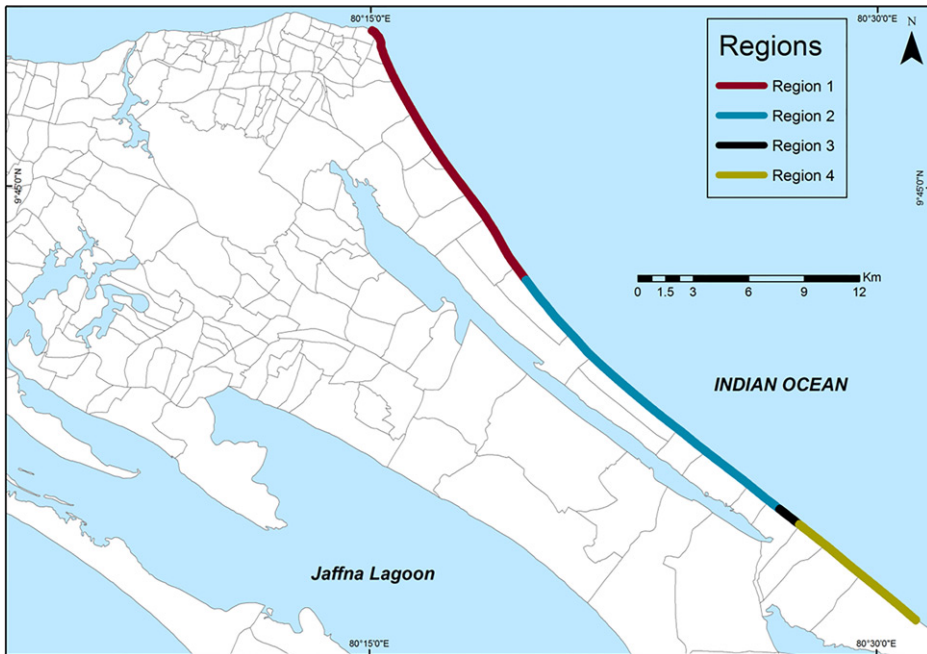


Figure 14. Categorized regions based on the available oldest and most recent shoreline.

Table 9. Details of each region.

Region	Year of oldest shoreline	Year of most recent shoreline	GN divisions	Shoreline length/km
1	2002	2017	Point Pedro East to Nagarkovil East	16.0
2	2003	2017	Nagarkovil East to Uduthurai	18.5
3	2006	2017	Uduthurai	1.3
4	2014	2017	Vetrilaikerny to Pokkaruppu	9.2

Table 10. Shoreline change statistics in each region.

	2002–2017 (Region 1)	2003–2017 (Region 2)	2006–2017 (Region 3)	2014–2017 (Region 4)
EPR	0.73 ± 0.66	0.33 ± 0.42	-0.16 ± 0.25	0.56 ± 2.66
SCE	21.85 ± 8.128	17.01 ± 4.37	9.9 ± 4.77	6.54 ± 4.48
NSM	10.97 ± 9.9	4.52 ± 5.81	-1.71 ± 2.62	1.62 ± 7.76
WLR	0.35 ± 0.65	0.16 ± 0.34	-0.1 ± 0.31	nil
WR2	0.26 ± 0.2	0.11 ± 0.12	0.15 ± 0.18	nil
WSE	1.81 ± 0.85	1.37 ± 0.33	1.28 ± 0.64	nil
SCE/Time	1.45	1.215	0.9	2.18

0.8 ± 0.2 and standard error of the estimate is 0.98 ± 0.67 m. 47.54% of the study area was responsible for this calculation.

The study found that there are four regions can be categorized based on the available oldest and most recent shoreline (Figure 14). First region (Region 1) represents the years in between 2002 and 2017 covering the GN Divisions from Point Pedro East to some part of Nagarkovil East. Second region (Region 2) represents the years in between 2003 and 2017 covering the GN Divisions from some part of the Nagarkovil East to Uduthurai.

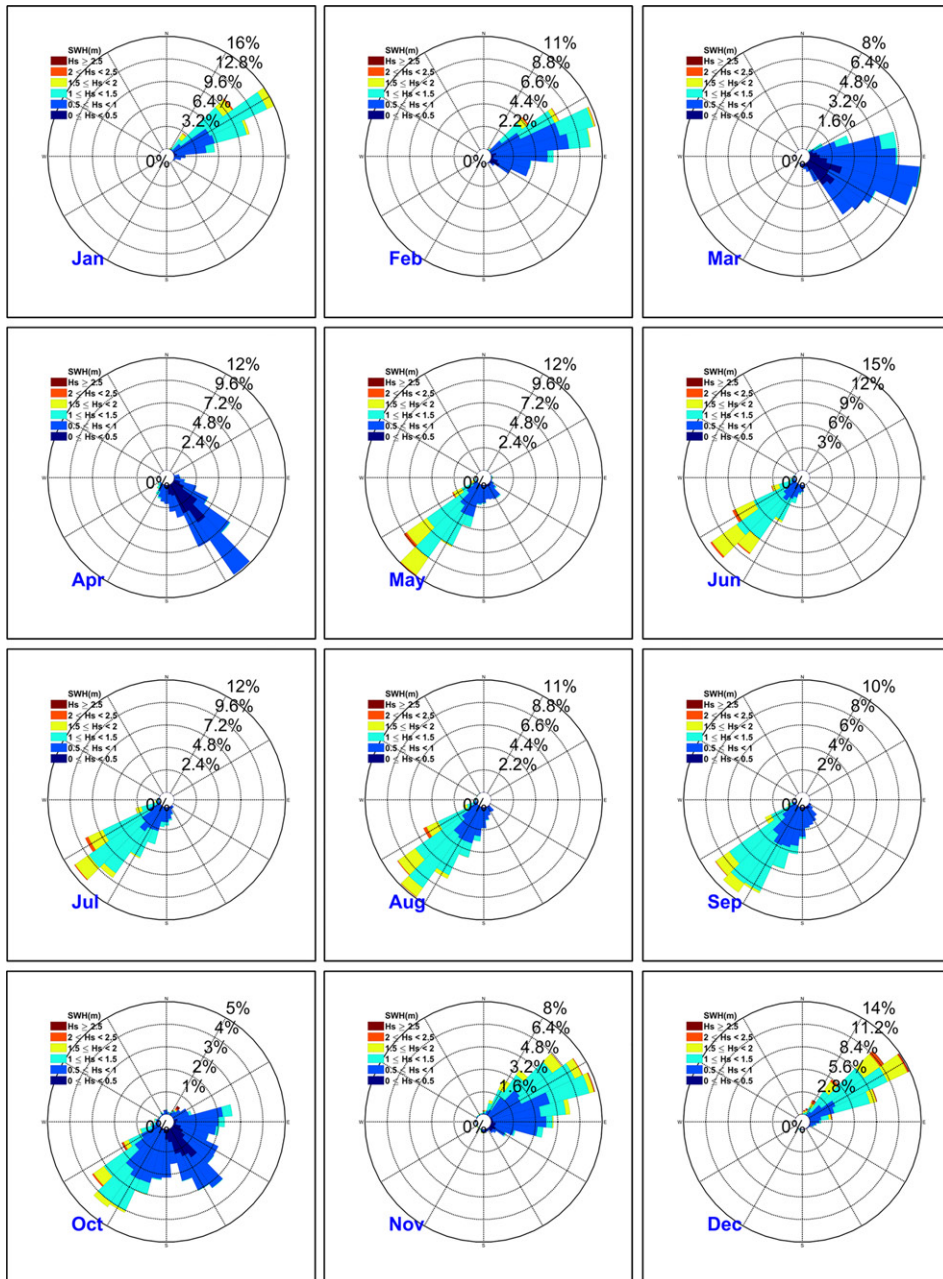


Figure 15. Wave Rose for north-east coast of Jaffna peninsula from January to December. (SWH = H_s = Significant Wave Height).

Third region (Region 3) from 2006 to 2017 represents the entire Uduthurai GN Division and the fourth region (Region 4) represents from 2014 to 2017 covering the GN Divisions from Vetrilaikerny to Pokkaruppu (Table 9).

The longest shoreline represents the region 2 (18.5 km) while the shortest shoreline represents the region 3 (1.3 km).

Table 11. Comparison of shoreline change statistics.

Change statistics	Season _not considered	Season _considered separately
NSM	6.13	5.25
EPR	0.50	0.90
SCE	16.59	9.84
WLR	0.24	0.75
WR2	0.18	0.55
WSE	1.56	1.12

Table 12. Pros and cons of each scenario.

	Season is not considered	Season is considered separately
Pros	Not affect the NSM, EPR as they are based on most recent and farthest shorelines Shoreline dynamism is well defined over the time Temporal resolution is high	Predictability is well defined. (High R^2 value) Low SE of the estimate of the regression analysis Inter-seasonal and intra-seasonal changes can be estimated
Cons	Predictability is not well defined. (Low R^2 value) High SE of the estimate of the regression analysis	Not effective under low data availability Temporal resolution is low

EPR and NSM analyses are very effective when only there are two shorelines. When there are more than two shorelines, they can be used in WLR analysis. Therefore, the shoreline change statistics were calculated separately for each category in order to have a better understanding of EPR and NSM including with some other relevant statistics. Results for this particular study are shown in the Table 10.

According to the above table it shows that the maximum EPR and NSM were given by the period from 2002 to 2017. Although the minimum NSM was given by the period from 2014 to 2017, the lowest EPR was shown during the period from 2006 to 2017. The EPR is somewhat higher in the period of 2014–2017 compared to the period of 2006–2017 because the time gap is higher in the latter scenario. Highest SCE was shown in the region 1 while the highest shoreline dynamism is shown by the region 4. WLR was also high in the Region 1 and it could not be calculated the WLR in the region 4 because there were only two shorelines used in the calculation. Therefore, the better interpretation of the shoreline change for the region 4 was given by EPR, SCE, and NSM. Because of that the shoreline change trend also could not be evaluated in this region. According to One-Way ANOVA, there is a significant difference of NSM, EPR, SCE, and WLR between regions ($P < 0.05$).

Figure 15 shows the wave rose for the study area for each month of the year. From November to February, the waves were directed to north-eastward and some of the waves with more than 2 m-wave height could be observed. This is the north-east monsoon period and sea is rough during this period. In the months of March and April, the sea is calm and wave height has kept less than 1.5 m in the direction of south-east. During the

period from May to September (south-west monsoon), the waves were directed towards south-west direction. A few waves have reached more than 2 m in height. In the month of October, the wave direction ranges from north-east to south-west.

Conclusion and recommendations

Overall north-east coastal belt of Jaffna peninsula is subjected to deposit while the sand-dune area is being increased. Accretion is very obvious adjacent to the breakwater and it is followed by erosion. Therefore, the human intervention such as construction of artificial barriers is directly influenced on the shoreline as it tends to alter. Although the coastal barriers contribute in the beach nourishment at particular area, as the beach sand is coming from the adjacent shore, some other area of the beach tends to erode. Therefore, coastal barriers are not always effective for coastal management. Since there are no any rivers in Jaffna peninsula, alluvial deposits are not contributed in the accretion process of the beach. Therefore, the sediment transportation could be mainly from the wave actions and surface currents which link with Bay of Bengal. During the south-west monsoon period there is a possibility to transport sediments to the beach via surface currents which are coming from east coast of India and directed towards the southern part of the country. The source for these sediments could be the east coast of India. In order to find the exact source of the sediments, further studies should be carried out. In addition, the wave actions which are prominent towards the beach in the south-west monsoon can transport the sediments and other calcium carbonate deposits such as corals and molluscan shells to the beach and contribute to the accretion process. In consideration of sand budget of the beach it is obvious that the incoming sediments are higher than the loosing sediments of the beach. Therefore, net accretion could be observed in the shoreline of the study area.

Limiting factors of the study are spatial and temporal gaps of the satellite data, cloud cover, lack of real time ground data and the accessibility restrictions for the dune area adjacent to the shoreline due to the risk of having hazardous materials remained as a repercussion of the civil war which prevailed over last few decades up to 2009. In such conditions, satellite remote sensing data play an important role to gather information in the places where the accessibility is restricted. Recently GE software had a rapid advancement and it provided high spatial resolution satellite images at temporal scales. Therefore, GE satellite images are ideal for time series analysis of shorelines after appropriate corrections. Besides, a very few studies have used GE satellite images for the coastal change analysis thereof this study guides how to use GE satellite images in an effective and efficient manner in

shoreline change detection. Other major advantages of using these images are cost effectiveness as they are freely available for certain years and appropriate for large scale shoreline change analysis (limited/local areas) with high accuracy. Therefore, the satellite images from GE platform are ideal for detecting shoreline change in a regional scale (large scaled maps). Low-resolution satellite images are not ideal to use to estimate the shoreline change detection as slight changes are not reflected well from that kind of analysis.

Major disadvantage of these images is having data gaps as the user has to satisfy with the data which is provided by the GE software and therefore temporal resolution of these data is low. When handling with GE satellite images RMS error under geometric correction, digitizing error, and tidal errors should be taken into consideration to ensure the accuracy of the delineated shoreline as it is a key factor of the accuracy of the analysis. All the shorelines should be digitized under same zooming level. In order to achieve this in GE, all the shorelines should be drawn under same eye-altitude to treat all shorelines same to minimize the digitizing errors. Overall idea about the shoreline change can be obtained even without considering the seasonal influences in the calculation up to a certain extent. But the shoreline is highly influenced by the monsoon pattern of Sri Lanka. The following table compares the mean shoreline change statistics under two scenarios namely, without and with consideration of season of the year (Table 11). This comparison concludes pros and cons of each scenario (Table 12). Accuracy of the shoreline change prediction can be increased by considering seasonal changes as the SE is reduced and predictability is also enhanced as the R^2 value is increased. Therefore, future prediction should be based on the seasonal changes since it has high R^2 value. Therefore, quantifying of seasonal changes is very important as there are significant changes of the shoreline among seasons. As far as the seasonal variation is concerned, the erosion is taken place in the north-east monsoon while the accretion is taken place in south-west monsoon. However, as the shoreline change rate estimation is influenced by the time gap between the most recent shoreline and the farthest shoreline, it gives more reliable results when the time gap is higher. Shoreline change values have slightly changed between two scenarios due to the shoreline data gaps.

Although the study did not focus on the influences of water currents, wave actions, wind patterns, and other climate variables, they should be taken into account for the better results under accuracy test. Irregularity of the shoreline due to the coastal morphological features such as bays, lagoons, estuaries, heads, spits, is one of the key factors which is also to be taken into consideration and this parameter is also to be tested and used in shorelines which are having high irregularities. SCATI index developed in this study is ideal for transect interval selection since this concept is not

well addressed in many shoreline change research studies with greater emphasis. However, this index is also to be further developed by considering aforementioned factors influenced on shoreline change and the technical aspect of the computers used in this regard. The information of the coastal erosion and accretion in this area will be effective for the stakeholders those who are engaging in coastal zone management such as coastal managers, coastal engineers, policy makers and the community to implement their day today activities and the management strategies. Further studies should be carried out to establish a proper mechanism to define predictability and the dynamic nature of the shoreline by developing shoreline change complexity index (SCCI) which can be used for the comparison of shorelines in various parts of the world.

Acknowledgements

We would like to convey our sincere thanks to the Ocean University of Sri Lanka for the facilities provided to prepare GIS maps, to collect remote sensing data including GCPs and for the library facilities. The support given by Mr. S. Suresh who is a government surveyor is highly appreciated for data collection for the beach slope analysis. Mr. Ruchira Jayathilaka who is working as a scientist in National Aquatic Resources Research and Development Agency, Sri Lanka also deserves the thanks as the support given by him in plotting the wave data.

Disclosure statement

No potential conflict of interest was reported by the authors.

Notes on contributors

All authors have contributed in the study by executing remote sensing & GIS data collection, processing, analyzing, statistical applications, map preparations and article writing by covering various aspects of the study.

ORCID

T. W. S. Warnasuriya  <http://orcid.org/0000-0001-8074-009X>

References

- Abeyasinghe P. B. n.d. "Limestone Resources of Sri Lanka." *Science Education Series*. n.d. *Limestone Resources of Sri Lanka*. Science Education Series. Natural Resources, Energy and Science Authority of Sri Lanka. <https://books.google.lk/books?id=D48dtwAACAAJ>.
- Appeaning Addo, K., P. N. Jayson-Quashigah, and K. S. Kufogbe. 2012. Quantitative analysis of shoreline change using medium resolution satellite imagery in keta, Ghana. *Marine Science* 1 (1):1–9. doi:10.5923/j.ms.20110101.01.

- Astrium. 2017. "Astrium to Provide Imagery for Google Maps and Google Earth _ UN-SPIDER Knowledge Portal." <http://www.un-spider.org/news-and-events/news/astrium-provide-imagery-google-maps-and-google-earth>.
- Bertacchini, E., and A. Capra. 2010. Map updating and coastline control with very high resolution satellite images: Application to Molise and Puglia coasts (Italy). *Italian Journal of Remote Sensing* 42 (2):103–15. doi:10.5721/ItJRS20104228.
- Boak, E. H., and I. L. Turner. 2005. Shoreline definition and detection: A review. *Journal of Coastal Research* 214:688–703. doi:10.2112/03-0071.1.
- Bouchahma, M., and W. Yan. 2012. Automatic measurement of shoreline change on Djerba island of Tunisia. *Computer and Information Science* 5 (5):17–24. doi:10.5539/cis.v5n5p17.
- Chand, P., and P. Acharya. 2010. Shoreline change and sea level rise along coast of Bhitarkanika wildlife sanctuary, Orissa: An analytical approach of remote sensing and statistical techniques. *International Journal of Geomatics and Geosciences* 1 (3):436–55.
- Chen, S.-S., L.-F. Chen, Q.-H. Liu, X. Li, and Q. Tan. 2005. Remote sensing and GIS-based integrated analysis of coastal changes and their environmental impacts in Lingding bay, pearl river estuary, South China. *Ocean and Coastal Management* 48 (1):65–83. doi:10.1016/j.ocecoaman.2004.11.004.
- Chenthamiselvan, S., R. S. Kankara, and B. Rajan. 2014. Assessment of shoreline changes along Karnataka coast, India using GIS & remote sensing techniques. *Indian Journal of Marine Sciences* 43:1286–1291.
- Cooper, J. A. G., D. W. T. Jackson, F. Navas, J. McKenna, and G. Malvarez. 2004. Identifying storm impacts on an embayed, high-energy coastline: Examples from Western Ireland. *Marine Geology* 210 (1–4):261–280. doi:10.1016/j.margeo.2004.05.012.
- Daniels, R. C. 2012. Using ArcMap to Extract Shorelines from Landsat TM & ETM + Data. Paper presented at the Thirty-Second ESRI International Users Conference Proceedings. 1–23. San Diego.
- Dayananda, H. V. 1992. "Shoreline Erosion in Sri Lanka's Coastal Areas." Colombo. Department of Census and Statistics. 2008. "Basic Population Information on Jaffna District – 2007." Colombo.
- Department of Meteorology Sri Lanka. 2016. "Climate of Sri Lanka." http://www.meteo.gov.lk/index.php?option=com_content&view=article&id=94&Itemid=310&lang=en.
- Dewidar, K. M., and O. E. Frihy. 2010. Automated techniques for quantification of beach change rates using landsat series along the. *Journal of Oceanography and Marine Science* 1:28–39.
- Digital Globe. 2017. "Our Constellation – DigitalGlobe." <https://www.digitalglobe.com/about/our-constellation#satellites&worldview-2>.
- District Secretariat Jaffna. 2016. "Annual Performance & Accounts Report." <https://www.parliament.lk/uploads/documents/paperspresented/performance-report-district-secretariat-jaffna-2016.pdf>.
- Dolan, R., M. S. Fenster, and S. J. Holme. 1991. Temporal analysis of shoreline recession and accretion. *Journal of Coastal Research* 7 (3):723–44.
- Fenster, M. S., R. Dolan, and R. A. Morton. 2001. Coastal storms and shoreline change: Signal or noise? *Journal of Coastal Research* 17 (3):714–20. <http://www.jstor.org/stable/4300222%5Cnhttp://www.jstor.org/stable/pdfplus/4300222.pdf>.
- Forbes, D. L., G. S. Parkes, G. K. Manson, and L. A. Ketch. 2004. Storms and shoreline retreat in the Southern Gulf of St. Lawrence. *Marine Geology* 210 (1–4):169–204. doi:10.1016/j.margeo.2004.05.009.
- Geeganage, G. T., and T. W. S. Warnasuriya. 2016. Shoreline change detection using remote sensing satellite data: Case study in selected area of Hambantota district, Sri

- Lanka. In *Scientific sessions*, ed. E.I.N. Silva. 107–9. Colombo: National Aquatic Resources Research and Development Agency.
- Gens, R. 2010. Remote sensing of coastlines: Detection, extraction and monitoring. *International Journal of Remote Sensing* 31 (7):1819–1836. doi:10.1080/01431160902926673.
- Genz, A. S., C. H. Fletcher, R. A. Dunn, L. N. Frazer, and J. J. Rooney. 2007. The predictive accuracy of shoreline change rate methods and alongshore beach variation on Maui, Hawaii. *Journal of Coastal Research* 231 (1):87–105. doi:10.2112/05-0521.1.
- Geological Survey Department, and Department of Mines and Energy South Australia. 1982. “Geological Map of Sri Lanka.” Colombo: Geological Survey Department.
- Google Earth Pro. 2017. “Jaffna, Sri Lanka. 9 49’ 36”N, 80 15’ 1”E, Eye Alt 500m.” Google. <https://www.google.com/earth/download/gep/agree.html>.
- Green, E. P., P. J. Mumby, A. J. Edwards, and C. D. Clark. 2000. *Remote sensing handbook for tropical coastal management*. Paris: UNESCO.
- Guariglia, A., A. Buonamassa, A. Losurdo, and R. Saladino. 2006. A multisource approach for coastline mapping and identification. *Annals of Geophysics* 49:295–304.
- Gunaalan, K., H. B. Asanthi, T. P. D. Gamage, M. Thushyanthy, and S. Saravanan. 2013. Geochemical variations of groundwater quality in coastal and karstic aquifers in Jaffna Peninsula, Sri Lanka. In *Management of water, energy and bio-resources in the era of climate change*, ed N. Janardhana Raju, W. Gossel, A. L. Ramanathan, and M. Sudhakar, 51–61. New Delhi: Capital Publishing Company. doi:10.1007/978-3-319-05969-3.
- Gunasekara, S. S., and N. Alahacoon. 2011. “Mapping of shoreline changes of selected sites of Jaffna Peninsula using satellite imagery.” *International symposium on agriculture and environment*. Matara: Faculty of Agriculture, University of Ruhuna.
- Himmelstoss, E. A. 2009. *Dsas 4.0 installation instruction and user guide*. Version 4.3. Reston: United States Geological Survey.
- Lee, J. S., and I. Jurkevich. 1990. Coastline detection and tracing in SAR images. *IEEE Transactions on Geoscience and Remote Sensing* 28 (4):662–668. doi:10.1109/TGRS.1990.572976.
- Lin, L., and P. Pussella. 2017. Assessment of vulnerability for coastal erosion with GIS and AHP techniques case study: Southern coastline of Sri Lanka. *Natural Resource Modeling* 30 (4): e12146.
- Lipakis, M., N. Chrysoulakis, and Y. Kamarianakis. 2005. “Shoreline Extraction Using Satellite Imagery.” *BEACHMED-e/OpTIMAL*, no. Beach Erosion Monitoring: 81–96.
- Liu, H., D. Sherman, and S. Gu. 2007. Automated extraction of shorelines from airborne light detection and ranging data and accuracy assessment based on monte carlo simulation. *Journal of Coastal Research* 236 (6):1359–1369. doi:10.2112/05-0580.1.
- Mahapatra, M., R. Ratheesh, and A. S. Rajawat. 2014. Shoreline change analysis along the coast of South Gujarat, India, using digital shoreline analysis system. *Journal of the Indian Society of Remote Sensing* 42 (4):869–876. doi:10.1007/s12524-013-0334-8.
- Makota, V., R. Sallem, and C. Mahika. 2004. Monitoring shoreline change using remote sensing and GIS: A case study of Kunduchi area, Tanzania. *Western Indian Ocean Journal of Marine Science* 3 (1):1–10.
- Malarvizhi, K., S. V. Kumar, and P. Porchelvan. 2016. Use of high resolution google earth satellite imagery in landuse map preparation for urban related applications. *Procedia Technology* 24 :1835–1842. doi:10.1016/j.protcy.2016.05.231.
- Morris, R. O. 1987. “Palk Strait and Palk Bay Eastern Part, Map, Scale 1-150000, No. 2197, Crown, Taunton.”
- Morton, R. A., T. Miller, and L. Moore. 2005. Historical shoreline changes along the US Gulf of Mexico: A summary of recent shoreline comparisons and analyses. *Journal of Coastal Research* 214 (4):704–709. doi:10.2112/04-0230.1.

- Mujabar, P. S., and N. Chandrasekar. 2013. Shoreline change analysis along the Coast between Kanyakumari and Tuticorin of India using remote sensing and GIS. *Arabian Journal of Geosciences* 6 (3):647–664. doi:10.1007/s12517-011-0394-4.
- Murray, N., S. Phinn, R. Clemens, C. Roelfsema, and R. Fuller. 2012. Continental scale mapping of tidal flats across east Asia using the landsat archive. *Remote Sensing* 4 (11): 3417–3426. doi:10.3390/rs4113417.
- Muthukumarasamy, R., M. V. Mukesh, M. Tamilselvi, S. R. Singarasubramanian, A. Chandrasekaran, and H. M. Sabeen. 2013. Shoreline changes using remotesensing and GIS environment: A case study of Valinokkam to Thoothukudi area, Tamilnadu, India. *International Journal of Innovative Technology and Exploring Engineering* 2 (6):72–75.
- Nandi, S., M. Ghosh, A. Kundu, D. Dutta, and M. Bakshi. 2016. Shoreline shifting and its prediction using remote sensing and GIS techniques: A case study of Sagar Island, West Bengal (India). *Journal of Coastal Conservation* 20 (1):61–80. doi:10.1007/s11852-015-0418-4.
- Natesan, U., N. Thulasiraman, K. Deepthi, and K. Kathiravan. 2013. Shoreline change analysis of Vedaranyam Coast, Tamil Nadu, India. *Environmental Monitoring and Assessment* 185 (6):5099–5109. doi:10.1007/s10661-012-2928-y.
- Niya, A. K., A. A. Alesheikh, M. Soltanpor, and M. M. Kheirkhahzarkesh. 2013. Shoreline change mapping using remote sensing and GIS, case study: Bushehr province. *International Journal of Remote Sensing Applications* 3 (3):102–107.
- Orford, J. D., D. L. Forbes, and S. C. Jennings. 2002. Organisational controls, typologies and time scales of paraglacial gravel-dominated coastal systems. *Geomorphology* 48 (1–3): 51–85. doi:10.1016/S0169-555X(02)00175-7.
- Pajak, M. J., and S. Leatherman. 2002. The high water line as shoreline indicator. *Journal of Coastal Research* 18 (2):329–337.
- Quashigah, P. N., K. A. Addo, and K. S. Kodzo. 2013. Medium resolution satellite imagery as a tool for monitoring shoreline change. Case study of the Eastern Coast of Ghana. *Journal of Coastal Research* 65:511–516. doi:10.2112/SI65-087.1.
- Reddy, M. A. 2008. *Remote sensing and geographical information systems*. BS publications. 3rd ed. Hyderabad: BS Publication. doi:10.1017/S0376892900039278.
- Sankar, S., V. Ravichandran, D. Venkatarao, and S. Badrinarayanan. 2014. Mapping of spatial and temporal variation of shoreline in Poompuhar using comprehensive approach. *Indian Journal of Marine Sciences* 43 (7):1292–1296.
- Sesli, F. A., F. Karsli, I. Colkesen, and N. Akyol. 2009. Monitoring the changing position of coastlines using aerial and satellite image data: An example from the Eastern Coast of Trabzon, Turkey. *Environmental Monitoring and Assessment* 153 (1–4):391–403. doi: 10.1007/s10661-008-0366-7.
- Shalaby, A., and R. Tateishi. 2007. Remote sensing and GIS for mapping and monitoring land cover and land-use changes in the Northwestern coastal zone of Egypt. *Applied Geography* 27 (1):28–41. doi:10.1016/j.apgeog.2006.09.004.
- Survey Department of Sri Lanka. 2007. *National atlas of Sri Lanka*. 2nd ed. Colombo: Survey Department of Sri Lanka.
- Thieler, E. R., J. F. O'Connell, and C. A. Schupp. 2001. The massachusetts shoreline change project: 1800s to 1994. *Technical Report T. USGS Adm Report NOAA*. <http://web.whoiedu/seagrant/wp-content/uploads/sites/24/2015/01/WHOI-T-01-001-Thieler-E.R.-The-Mass.-Shorel.pdf>.
- Van, T. T., and T. T. Binh. 2009. Application of remote sensing for shoreline change detection in Cuu Long Estuary. *VNU Journal of Science, Earth Sciences* 25:217–222.

- Warnasuriya, T. W. S. 2015. Mapping land-use pattern using image processing techniques for medium resolution satellite data: Case study in Matara District, Sri Lanka. In *International conference on advances in ICT for emerging regions (ICTer)*. 106–111. Colombo: IEEE. doi:10.1109/ICTER.2015.7377674.
- Warnasuriya, T. W. S., P. B. T. Pradeep Kumara, and N. Alahacoon. 2015. Mapping of selected coral reefs in Southern, Sri Lanka using remote sensing methods. *Sri Lanka Journal of Aquatic Sciences* 19:41–55. doi:10.4038/sljas.v19i0.7450.
- Weerakkody, U. 1995. *Changing coastline of southwest Sri Lanka*. Colombo: Natural Resources, Energy & Science Authority of Sri Lanka. http://thakshana.nsf.ac.lk/slstic/NA-03/NA_3_i.pdf.
- White, K., and H. M. El Asmar. 1999. Monitoring changing position of coastlines using thematic mapper imagery, an example from the Nile Delta. *Geomorphology* 29 (1–2): 93–105. doi:10.1016/S0169-555X(99)00008-2.
- White, S. A., and Y. Wang. 2003. Utilizing DEMs derived from LIDAR data to analyze morphologic change in the North Carolina coastline. *Remote Sensing of Environment* 85 (1):39–47. doi:10.1016/S0034-4257(02)00185-2.
- Zhao, B., H. Guo, Y. Yan, Q. Wang, and B. Li. 2008. A simple waterline approach for tidalands using multi-temporal satellite images: A case study in the Yangtze Delta. *Estuarine, Coastal and Shelf Science* 77 (1):134–142. doi:10.1016/j.ecss.2007.09.022.